CHALMERS

Optimizing Coordinated Multi-Point Transmission under Unreliable Backhaul

Master's Thesis in Communication Engineering

ZOLTÁN MAYER

Department of Signals and Systems
Division of Communication Systems
CHALMERS UNIVERSITY OF TECHNOLOGY
Gothenburg, Sweden 2013
Master's thesis EX001/2013

MASTER'S THESIS IN COMMUNICATION ENGINEERING

Optimizing Coordinated Multi-Point Transmission under Unreliable Backhaul

ZOLTÁN MAYER

Department of Signals and Systems
Division of Communication Systems
CHALMERS UNIVERSITY OF TECHNOLOGY
Gothenburg, Sweden 2013

Optimizing Coordinated Multi-Point Transmission under Unreliable Backhaul
ZOLTÁN MAYER

Master's Thesis EX001/2013
Department of Signals and Systems
Division of Communication Systems
Chalmers University of Technology
SE-412 96 Gothenburg
Sweden
Telephone: + 46 (0)31-772 1000

Department of Signals and Systems
Gothenburg, Sweden 2013

Abstract

Coordinated Multi-Point (CoMP) transmission entails that a number of base stations (BSs) share information and jointly act to mitigate inter-cell interference. All CoMP techniques rely on information exchange between BSs through the backhaul network, i.e., a network interconnecting BSs. This information can be user channel state information (CSI), user scheduling decisions and user data. Therefore the quality of backhaul links in terms of capacity, latency and reliability is crucial for CoMP, i.e., the performance of CoMP schemes can be compromised if the backhaul links are unreliable. In Heterogeneous Networks (HetNet) deploying high numbers of small cells to complement improved and densified macrocell layers will require new mobile backhaul solutions apart from the dedicated high-performance backhaul. The use of lower-performance backhaul options and the reuse of existing resources on site will be necessary as such as Non-line-of-sight (NLOS) microwave links and public DSL networks. The purpose of this Master thesis is to investigate the performance of various CoMP schemes under unreliable backhaul. The thesis involves modelling of an unreliable wireless backhaul network. An important question that the thesis addresses is to what degree different CoMP schemes suffer from unreliable backhaul. More importantly the thesis focuses on optimizing the mode of CoMP operation as a function of the backhaul reliability.

Key words: coordinated multi-point (CoMP), heterogeneous networks (HetNet), backhaul reliability, control channel, link failure probability

Contents

Acknowledgements

I am grateful to all the people who made this thesis work possible.

I wish to thank my examiner Tommy Svensson, and my supervisors Agisilaos Papadogiannis and Jingya Li for giving me the opportunity to work with them on such an interesting topic. Their guidance was invaluable, and I learned them to be not only accomplished specialists but excellent educators too.

In addition, I would like to express my gratitude to all the staff at Chalmers, studying in Gothenburg was a very rewarding experience.

I am also thankful to my parents and friends for their encouragement and support.

Acronyms

3GPP	3rd Generation Partnership Project
CS	Coordinated scheduling
CSG	Closed subscriber group
CSI	Channel state information
CoMP	Coordinated multi-point transmission
eNB	Evolved Node B
HeNB	Home evolved Node B
HetNet	Heterogeneous network
ICIC	Inter-cell interference coordination
ITU	International Telecommunication Union
JT	Joint transmission
LFP	Link failure probability
LTE	Long-term evolution
M2M	Machine to machine
MIMO	Multiple-input and multiple-output
NLOS	Non-line-of-sight
PtMP	Point-to-multipoint
RAN	Radio access network
TN	Transmission node
UE	User equipment
W-CDMA	Wideband code division multiple access

I. Overview

1 Introduction and motivation

New, powerful mobile devices like smartphones and tablets are spreading fast, and customers need and expect to have ubiquitous broadband access to online services. A single smartphone or a single tablet can generate as much traffic as 35 or 121 basic-feature phones respectively. Overall mobile data traffic is expected to grow to 10.8 exabytes per month by 2016, an 18-fold increase over 2011 (Fig. 1) [1]. Not only connected people, but connected things also contribute to this growth, as the number of mobile machine-to-machine (M2M) connections may cross 200 million globally by 2014 [2].

To answer the challenge of providing significantly faster wireless data transfer speeds, Long Term Evolution (LTE) was developed by the Third Generation Partnership Project (3GPP). LTE is now growing strongly, with 13 million new subscriptions added in Q3 2012 and will reach around 1.6 billion subscriptions in 2018. (Fig. 2) [3].

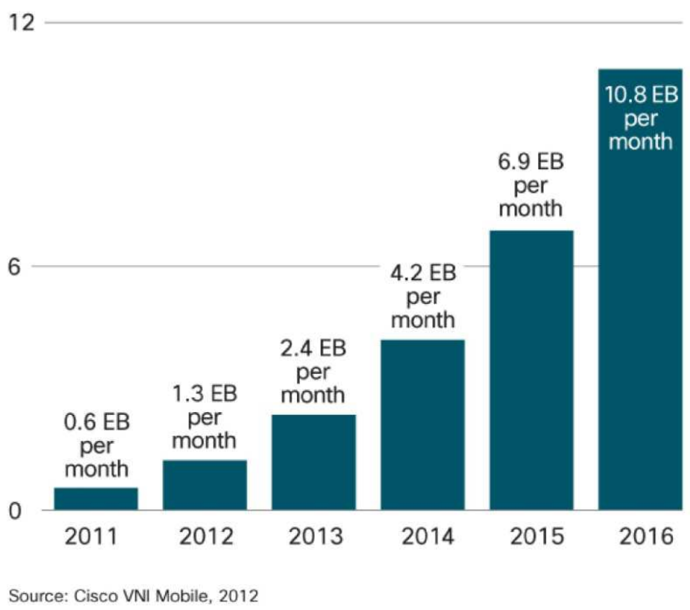

Figure 1. Exabytes per month of mobile data traffic by 2016 [1]

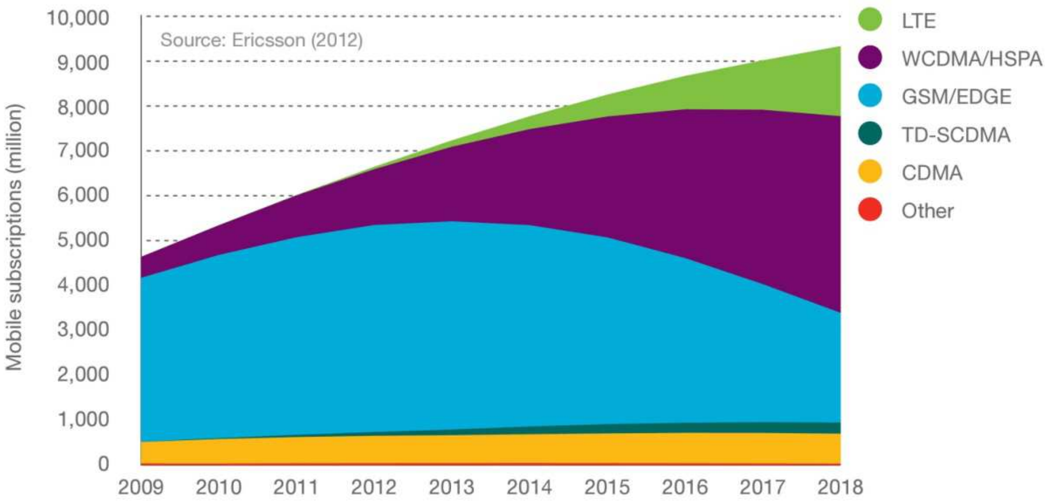

Figure 2. Mobile subscriptions by technology, 2009-2018 [3]

Release 10 of the standard, also known as LTE-Advanced, is of particular interest as it is the major technology approved by the International Telecommunications Union (ITU) as fulfilling the complete set of requirements for the fourth generation of mobile phone communications standards (4G).

The evident way to increase capacity is to apply new spectrum to telecommunications and/or improve spectral efficiency per link. However, radio spectrum has become a scarce commodity and spectral efficiency per link is already approaching theoretical limits. To cost-effectively increase the capacity of cellular wireless networks, a paradigm shift in infrastructure deployment is necessary. In order to improve network capacity, new deployment strategies have emerged based on a heterogeneous network (HetNet) topology that blends macrocells with smaller, low-power cells (i.e. pico and femto cells), and relays. HetNet technology is focused on improving spectral efficiency per unit area. Heterogeneous networks are expected to be an integral component of future LTE network deployments and Ericsson has projected that by 2017 each urban macro base station will be complemented by an average of 3 small cells [3]. In practice, a small cell unit can look like a WiFi access point; however, it also includes all the core network elements.

Even though the deployment of low power access points can improve achievable wireless data rates, these benefits are accompanied by several technical and economic challenges. The most prominent technical challenge is co- and cross-tier interference. Interference can be mitigated by cooperation between neighboring cell sites. Recently such techniques are referred to as Coordinated Multi-Point (CoMP) [4]. CoMP schemes allow interference mitigation through joint and coherent transmission from multiple TNs, but at the cost of increased complexity and other signalling overhead [5]. The Coordinated Multi-Point Operation feature for the LTE standard is currently being developed by 3GPP and will be included in Release 11 [6].

To fully exploit the performance gain offered by HetNets and CoMP, highly reliable backhaul links are required for interconnecting the cell sites and the core network. However, building high quality wireline backhaul is expensive; therefore, an economically viable solution is to reuse existing infrastructure, e.g. digital subscriber lines. Moreover, CoMP solutions are also sensitive to various other factors, such as the network structure.

In this thesis, the problem of CoMP transmission under unreliable backhaul is addressed. Motivated by the HetNet scenario, a cluster of cooperative homogeneous nodes with unreliable backhaul links has been studied. My goal was to find a way to assess the performance of different CoMP schemes. Two metrics were taken into consideration: the probability of backhaul failure impeding transmission in a cooperative cluster, and the achievable sum rate in a cooperative cluster. System models are introduced for different CoMP schemes and network architectures, analytical expressions are given for the event of failure in a cooperative cluster and the achievable sum rates are compared by simulation.

2 Heterogeneous networks in LTE-advanced

2.1 Traditional access network deployment

Until recently, wireless cellular networks were typically deployed as homogeneous networks, and the planning process was centered around macro base stations. In such a homogeneous network all cell sites have approximately the same characteristics, most importantly similar transmit power levels. The location of the cell sites is chosen with meticulous planning, in order to provide good coverage and to avoid interference as much as possible. However, such networks cannot meet the present-day demand for data traffic capacity, because the spectral efficiency per link has practically reached its theoretical limit [7]. Densifying the macro layer offers some gain, but the benefits are limited by interference.

2.2 The emergence of the small cell

Since wireless spectrum is very expensive, spatial frequency re-use is the most viable solution to provide higher throughput. This can be achieved by splitting cell sites and reducing transmit power levels. Low power nodes can be deployed in existing macro cell networks, for example at cell edges and in congested network areas. Such a heterogeneous network configuration (HetNet) can support high data rates, if configured properly. Standardized by 3GPP, LTE HetNets consist of the following elements:

- Macrocells: traditional base stations, enhanced NodeBs (eNBs) in LTE. Installed by the operator, these base stations provide essential coverage, and typically use a dedicated backhaul.

- Picocells: have similar features as macrocells, but lower transmit power, thus smaller coverage area. In a typical scenario, picocells are deployed in capacity starved locations, and can be accessible to all cellular users.

- Relays: Relay stations can be deployed to improve reception in poor coverage areas. They forward an enhanced version of the received signal between macro base stations and mobile stations. Relays don’t require wireline backhaul.

- Femtocells: These base stations are called Home eNodeBs (HeNB) in LTE, and are usually deployed indoors in a home or small office environment. Typically, femtocells are privately owned and under closed subscriber group (CSG) operation, where only restricted users are granted permission to access. These access points can utilize existing broadband connections as backhaul links.

The main characteristics of HetNet infrastructure elements are summarized in Table 1 [8].

	Transmit power	Coverage	Backhaul
Macrocell	45dBm	1000m	S1 interface
Picocell	30dBm	< 300m	X2 interface
Relay	30dBm	300m	Wireless
Femtocell	< 25dBm	< 50m	xDSL

Table 1. The elements of HetNet infrastructure

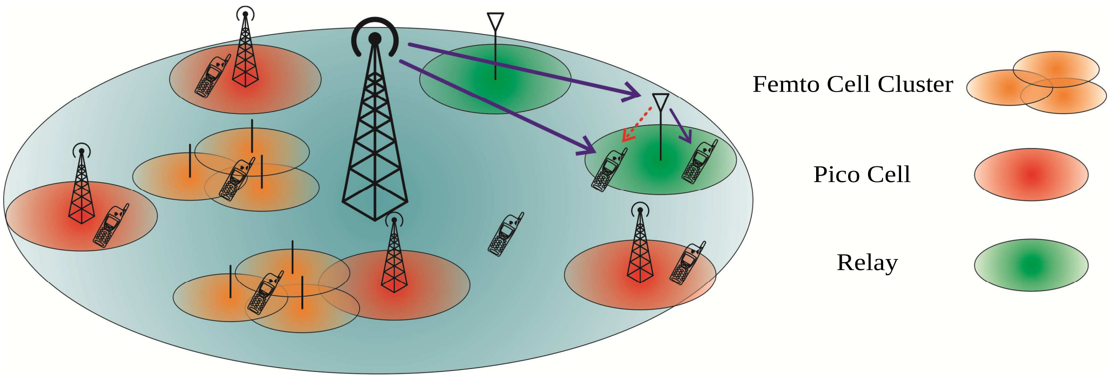

Figure 3. Heterogeneous network topology

A key concept in HetNets is range expansion, which allows user terminals to benefit from being associated to a low-power base stations while inside the coverage area of a macro station [9]. Traditionally, user terminals connect to the base station from which the strongest signal can be received. This is not necessarily the best strategy, since the user terminal might connect to a macro station even if the path loss towards a low-power station is lower. By adding an offset in the user terminal to the received signal strength from the macro node, the uptake area of the low-power node can be expanded. Range expansion is already possible in the first release of LTE, Rel-8 [10].

2.3 Technical challenges

The standards that make HetNet deployment possible are under development today. Without attempting to be comprehensive, the main problem in HetNets appears to be interference. Motivated by the pursuit for the best solution, multiple technologies are being heavily researched. In traditional networks, where all parts of the infrastructure are deployed by the operator, networks frequency reuse schemes are successfully used to mitigate interference. In HetNets, however, such schemes cannot be applied for multiple reasons. Firstly, due to the potentially large number of low-power cells and limited radio spectrum, collisions cannot be avoided. Secondly, user-deployed femtocells will render centralized frequency planning increasingly challenging.

3 Coordinated multi-point transmission in LTE-advanced

3.1 Using network MIMO to combat interference

In Release 8 multiple-input multiple-output (MIMO) technologies are adopted by LTE to address demand for higher data rates. Intercell interference coordination (ICIC) techniques are also supported focusing on homogeneous networks.

In LTE-Advanced HetNet deployments present a new set of problems. With the co-existence of base stations with different transmit power levels new interference scenarios need to be considered. Deployment of large numbers of low-power cells in the future limits the feasibility of centralized radio resource management.

To address the challenge of interference in HetNets, the possibility of network-level MIMO by means of tight cooperation between a set of network nodes is heavily researched. Such emerging techniques are to be included in the future releases of LTE, and are referred to as coordinated multi-point transmission (CoMP). Various CoMP schemes are candidates for standardization, all of which use channel state information (CSI) to perform scheduling and precoding decisions.

3.2 Overview of CoMP techniques

Support of CoMP in future releases of LTE is targeted by 3GPP [11]. Downlink CoMP schemes can be classified into several categories, in this work the two following schemes are considered:

- Coordinated scheduling (CS): all UEs are served by only one cell, therefore, user data is only available at the serving cell, but scheduling decisions are aligned across cooperating cell sites.

- Coherent joint transmission (JT): multiple cell sites transmit simultaneously to a single UE in the cooperating cluster, therefore, user data needs to be available at several cell sites. The UEs combine coherently all received signals at symbol level. For this technique to work, tight time and phase synchronization amongst the cooperating cell sites is required [12].

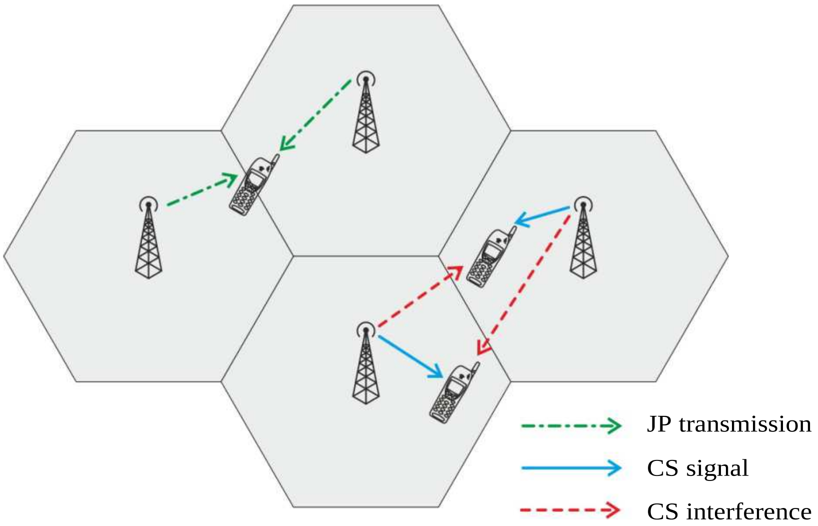

Figure 4. Joint Processing and Coordinated Scheduling for downlink CoMP

Uplink CoMP will also be a part of LTE, however, such techniques are left outside the scope of the present work.

3.3 Technical challenges

Since all CoMP schemes depend on information exchange between the cell sites in the cooperating clusters, the quality of the backhaul network is of high importance. The JT scheme offers the highest performance gain, however, it requires user data to be present at all cooperating cell sites, and thus high capacity backhaul links are needed. Low latency is crucial for all CoMP schemes, since CSI aging degrades the performance of the system.

Deploying a high quality backhaul network would overcome these limitations, but it is not economically viable. The reuse of existing, lower quality backhaul solutions is also required to make the HetNet concept successful, where large numbers of low-power nodes are deployed without central planning.

4 Deployment status of small cell networks

4.1 Current developments

LTE is the fastest-developing system in the history of mobile communications in terms of buildout and uptake. LTE is currently being deployed and built out in all regions, and the number of total subscriptions reaches around 55 million at the end of 2012 [3].

The Small Cell Forum, formerly known as the Femto Forum, supports the wide-scale adoption of small cells. The Small Cell Forum is directed by an executive board inclusive of all major stakeholders in the telecommunications equipment market [13]. The Small Cell Forum takes part in 3GPP as a Market Representation Partner [3gpp]. Along with the development of LTE standardization in 3GPP, telecommunications equipment providers shape their portfolio to support the latest features.

Ericsson completed its acquisition of BelAir Networks, a North American carrier-grade Wi-Fi company in April 2012 [14]. With the accelerated integration of Wi-Fi and other cellular technologies the company aims to strengthen its HetNet offering.

Qualcomm announced in August 2012 that it has acquired DesignArt Networks, a leader in small cell modem and system design for cellular base stations. DesignArt’s technology also offers integrated line-of-sight and non-line-of-sight wireless backhaul to reduce the cost of outdoor small cell deployments [15].

Nokia Siemens Networks offers the Flexi Zone suite as a combined

3G/LTE/Wi-Fi-capable cellular solution engineered to offload traffic from the macro network [16]. Flexi Zone has won the Best of 4G Awards Radio Access Network (RAN) and Small Cell Technology Product category [17]. Nokia Siemens Networks has been selected by O2 to prepare its network to deliver LTE services across London and the South East of England [18].

Alcatel-Lucent's small cells portfolio was showcased with the first live, commercial deployment of an LTE HetNet at the Mobile World Congress in Barcelona in February 2012. The network provided speeds of up to 10 times those offered by a 3G network. The company claims that this type of network uses 35 percent less power and delivers a 50 percent total cost of ownership savings, compared to conventional macro cell deployments [19].

Cisco Systems revealed in an interview that it will eventually round out its small-cell portfolio with the introduction of an LTE-capable base station. "We are now entering the post-macrocell era, where small cells also will play a critical role in delivering the next-generation mobile Internet," said John Chambers, Cisco chairman and CEO [20].

AT&T announced that it will also use more than 40,000 small cells to build out a highly dense network. The initial deployments of these dense networks will begin in the first quarter of 2013 and will work with the 3G UMTS and HSPA+ networks that AT&T has deployed. By 2014 AT&T will support LTE on these small cells as well [21].

NTT DoCoMo announced in November 2012 that it has developed the world's first dual-mode femtocell, supporting 3G (W-CDMA) and LTE simultaneously for improved service coverage in indoor locations such as offices, shops and homes. The dual-mode femtocell will be commercially launched from December 2012 [22].

Femtocells and small cells became buzzwords, and according to Informa Telecoms & Media's estimates, the number of small cells deployed overtook the total number of macro cells between October-November 2012. Informa's report estimates that the number of small cells has surpassed 6 million while there are 5.9 million macrocells deployed. The majority of these, however, are using 3G technology and the only one third of the total units shipped will be 4G small cells in 2013 [23].

4.2 Heterogeneous backhaul solutions

Although LTE small cell deployments are already on their way, the full potential of the HetNet concept can only be realized with utilizing CoMP transmission to overcome interference. CoMP technology itself, however, is yet to be standardized, and before it can be introduced to live systems, wireless network operators and equipment providers will need to find a way to support its increased backhaul requirements. The effects of constrained backhaul on HetNets and CoMP transmission in particular is a heavily researched area [24-26]. Researchers also focus on developing schemes that reduce the strain on backhaul links without performance degradation [27-29].

In order to reduce installation and operating expenses, the use of existing infrastructure is to be considered. With in-building applications, availability of Ethernet reduces the complexity. Outdoor cells, however, may not have access to wired Ethernet connectivity. Alternatively, non-line of sight (NLOS) RF-based backhaul can be used to carry the traffic.

In 2011 wireless backhaul solution provider Siklu has closed a $19 million investment round led by Qualcomm and Amiti Ventures [32]. Siklu's gigabit wireless backhaul solutions operate on the licensed E-band wireless spectrum and support next generation 4G/LTE [33].

Sub10 Systems is a fast-growing developer and manufacturer of point-to-point millimetre wave radio links designed for mobile operator small cell backhaul networks. In September 2012 the company announced signing a global supply and distribution agreement with Alcatel-Lucent [34].

Virgin Media carried out an initial trial in London with Airspan's AirSynergy small cell LTE architecture. AirSynergy supports LTE-Advanced network deployments, providing a small cell layer in advanced HetNets. The solutions offers efficient, low latency integrated NLOS wireless backhaul [36].

Huawei launched its wireless small cell backhaul solution in May 2012 under the brand name eRelay. It utilizes NLOS transmission and supports LTE technology with Point-to-Multipoint (PtMP) transmission [35].

Market research firm Infonetics Research expects a cumulative $5 billion to be spent worldwide on outdoor small cell backhaul equipment between 2012 and 2016, with the market kicking into high gear in 2014. According to the report significant shifts are expected in the type of equipment vendors use to backhaul outdoor small cells, with millimetre wave and non-line-of-sight equipment becoming the top segments of the market by 2016 [30]. A brief overview of wireless backhaul options is shown in Table 2.

	mm Wave 60 GHz	**E-Band 70-80 GHz**	**Sub-6 GHz**
Main pros	Unlicensed, higher capacity, high frequency re-use factor	Inexpensive license, higher capacity	Both LoS and NLoS solutions
Main cons	Requires LoS, very short links	Requires LoS	**Licensed sub 6 GHz:** Expensive, medium capacity **Unlicensed sub 6 GHz:** Medium capacity
Capacity	Multi Gbps	1.2 Gbps	200 Mbps Aggregated
Backhaul licensing	Unlicensed	Light License	Licensed (3.5 GHz) and Unlicensed
Line of Sight	LoS only	LoS only	LoS / NLoS

Table 2. Wireless backhaul alternatives for small cells [31]

5 Contributions

5.1 Paper A - On the Impact of Backhaul Channel Reliability on Cooperative Wireless Networks

In this paper, motivated by the HetNet scenario, we evaluate the downlink of a cooperative wireless network, and study the impact of backhaul channel reliability on the system performance. A backhauling model is introduced for the cooperative systems under different network architectures, i.e., the centralized and semi-distributed versions. An analytical approach is taken to investigate how backhaul reliability affects the operation of the cooperating TNs. Under each considered network CoMP architecture, the zero-forcing joint transmission scheme and the multi-point coordinated scheduling scheme are studied and compared. We have found that although higher rates are achievable with joint transmission, it is more sensitive to backhaul link failure.

5.2 Paper B - On the Impact of Control Channel Reliability on Coordinated Multi-Point Transmission

As an extension of the work done in Paper A, the impact of control channel reliability on the system performance with different CoMP techniques is studied. A backhauling model is introduced for an additional network architecture, the fully distributed version. An analytical approach is taken to investigate how backhaul and access link reliability affects the operation of the cooperating TNs. We provide general closed-form expressions to assess the probability of a TN staying silent in a resource slot, depending on the LFPs of the backhaul network and the access links. Under each considered network CoMP architecture, the zero-forcing coherent joint transmission scheme and the multi-point coordinated scheduling scheme are studied and compared. We have found that the semi- and fully distributed architectures are more robust to link failure, as the performance of the CoMP schemes under these architectures will converge to traditional single cell transmission, as the probability of link failure grows.

6 Future work

To study the effects of constrained backhaul on CoMP, mathematical models of different types of backhaul should be introduced. Copper, fibre and microwave backhaul solutions have different characteristics, which in turn alter the operation of the cooperative cluster in different ways.

This work only deals with a reduced set of downlink CoMP schemes. Additional schemes can be investigated including uplink CoMP and novel schemes that were developed having regard to imperfect backhaul.

This work focuses on the unreliable nature of backhaul links in HetNets, by analyzing a cluster of homogeneous nodes. As an extension to this work, clusters of nodes with different transmission power and cell size can be studied. Improved simulations can be performed with commercially available software, for realistic LTE HetNet scenarios. As the new releases of LTE will support standardized CoMP schemes, pragmatical simulation of a complete network becomes possible.

7 References

[1] "Cisco Visual Networking Index: Global Mobile Data Traffic Forecast Update, 2011–2016," available at: http://www.cisco.com/en/US/solutions/collateral/ns341/ns525/ns537/ns705/ns827/white_paper_c11-520862.pdf (accessed 31 December 2012)

[2] Berg Insight, "The Global Wireless M2M Market - 4th Edition," product sheet available at: http://www.berginsight.com/ReportPDF/ProductSheet/bi-globalm2m4-ps.pdf (accessed 31 December 2012)

[3] "Ericsson Mobility Report, November 2012," available at: http://www.ericsson.com/res/docs/2012/ericsson-mobility-report-november-2012.pdf (accessed 31 December 2012)

[4] RY. H. Nam, L. J. Liu, Y. Wang, C. Zhang, J. Cho and J. K. Han, "Cooperative communication technologies for LTE-Advanced" *IEEE ICASSP 2010*, pp. 5610–5613, Mar. 2010.

[5] F. Pantisano, M. Bennis, W. Saad, M. Debbah, M, Latva-aho, "On the Impact of Heterogeneous Backhauls on Coordinated Multipoint Transmission in Femtocell Networks," *IEEE ICC 2012*, Ottawa, Canada, Jun. 2012.

[6] "3GPP TR 36.819 Coordinated multi-point operation for LTE physical layer aspects," available at: http://www.3gpp.org/ftp/Specs/html-info/36819.htm (accessed 31 December 2012)

[7] CP. Mogensen, W. Na, I. Kovacs, F. Frederiksen, A. Pokhariyal, K. Pedersen, T. Kolding, K. Hugl, and M. Kuusela, "LTE capacity compared to the Shannon bound," *IEEE VTC 2007*, pp. 1234–1238, Dublin, Apr. 2007.

[8] C D. López-Pérez, ˙I. Güvenç, G. de la Roche, M. Kountouris, T. Q. Quek, and J. Zhang, "Enhanced intercell interference coordination challenges in heterogeneous networks," *IEEE Wireless Commun. Mag.*, vol. 18, no. 3, pp. 22–30, Jun. 2011.

[9] Asif Ali Khan, "Interference Management for Heterogeneous Networks in 3GPP LTE Advanced and Beyond," *MSc thesis*, The Royal Institute of Technology, Stockholm, Sweden, Dec. 2011.

[10] S. Parkvall, E. Dahlman, G. Jöngren, S. Landström and L. Lindbom, “Heterogeneous network deployments in LTE,” *Ericsson Review*, 2011.

[11] “3GPP TR 36.814 Evolved Universal Terrestrial Radio Access (E-UTRA); Further advancements for E-UTRA physical layer aspects,” available at: http://www.3gpp.org/ftp/Specs/html-info/36814.htm (accessed 31 December 2012)

[12] Tran, Thien-Toan, Yoan Shin, and Oh-Soon Shin. “Overview of enabling technologies for 3GPP LTE-advanced,” *EURASIP Journal on Wireless Communications & Networking*, 2012.

[13] “Small Cell Forum – Who are we,” available at: http://www.smallcellforum.org/aboutus-who-are-we (accessed 31 December 2012)

[14] Press release, “Ericsson completes acquisition of BelAir Networks,” available at: http://hugin.info/1061/R/1598985/504523.pdf (accessed 31 December 2012)

[15] Press release, “Qualcomm Acquires Small Cell Pioneer DesignArt Networks,” available at: http://www.qualcomm.com/media/releases/2012/08/23/qualcomm-acquires-small-cell-pioneer-designart-networks (accessed 31 December 2012)

[16] NSN portfolio, “Cost-effective capacity to weather the data storm,” available at: http://www.nokiasiemensnetworks.com/portfolio/solutions/heterogeneous-networks/flexi-zone (accessed 31 December 2012)

[17] Press release, “Best of 4G Awards Winners Announced at 4G World 2012,” available at: http://www.4gworld.com/chicago/news/#id_10302012 (accessed 31 December 2012)

[18] Comms Business, “Nokia Siemens Networks prepares O2’s network for LTE in the UK,” available at: http://www.commsbusiness.co.uk/RSS_News_Articles.cfm?NewsID=18437 (accessed 31 December 2012)

[19] Press release, “Telefonica Unveils Smart 4G Experience at Mobile World Congress,” available at: http://tinyurl.com/AlcatelSmart4G (accessed 31 December 2012)

[20] Light Reading Mobile News, "Cisco Works With AT&T Et Al on First Small Cell," available at: http://www.lightreading.com/document.asp?doc_id=218092 (accessed 31 December 2012)

[21] Press release, "AT&T to Invest $14 Billion," available at: http://www.att.com/gen/press-room?pid=23506&cdvn=news&newsarticleid=35661 (accessed 31 December 2012)

[22] Press release, "DOCOMO Develops World's First Small-cell Base Station for 3G and LTE," available at: http://www.nttdocomo.com/pr/2012/001620.html (accessed 31 December 2012)

[23] White paper, "Small Cell Market Status – December 2012," available at: http://www.smallcellforum.org/resources-white-papers (accessed 31 December 2012)

[24] P. Marsch and G. Fettweis, "On downlink network MIMO under aconstrained backhaul and imperfect channel knowledge," *IEEE GlobeCom 2009*, Honolulu, Hawaii, Dec. 2009.

[25] A. Chowdhery, W. Yu, and J. M. Cioffi, "Cooperative wireless multicell OFDMA network with backhaul capacity constraints," *IEEE ICC 2011*, Kyoto, Japan, June 2011.

[26] R. Zakhour and D. Gesbert, "Optimized data sharing in multicell MIMO with finite backhaul capacity," *IEEE Trans. Signal Processing*, vol. 59, no. 12, pp. 6102–6111, Dec. 2011.

[27] Zhang, Qian, Chenyang Yang, and Andreas F. Molisch. "Cooperative downlink transmission mode selection under limited-capacity backhaul," *IEEE WCNC 2012*, Beijing, China, Apr. 2012.

[28] J. Li, A. Papadogiannis, R. Apelfröjd, T. Svensson, and M. Sternad, "Per-formance Evaluation of Coordinated Multi-Point Transmission Schemes with Predicted CSI," *IEEE PIMRC 2012*, Sydney, Australia, Sep. 2012.

[29] A. Papadogiannis, H. J. Bang, D. Gesbert and E. Hardouin, "Efficient selective feedback design for multicell cooperative networks," *IEEE Trans. Vehicular Techn.*, vol. 60, no. 1, pp. 196–205, Jan. 2011

[30] Israel Science Technology News, “Ethernet wireless backhaul solution provider Siklu raises $19 million,” available at: http://israelsciencetechnology.blogspirit.com/archive/2011/10/20/ethernet-wireless-backhaul-solution-provider-siklu.html (accessed 31 December 2012)

[31] Siklu product portfolio, “The Etherhaul E-Band Millimeter Wave Radio,” available at: http://www.siklu.com/products.html (accessed 31 December 2012)

[32] Press release, “Sub 10 Systems technology to be offered by Alcatel-Lucent,” available at: http://www.sub10systems.com/news/2012/09/sub-10-systems-technology-to-be-offered-by-alcatel-lucent-as-part-of-its-microwave-wireless-transmission-portfolio/ (accessed 31 December 2012)

[33] Press release, “Virgin Media Trials Airspan’s Small-Cell LTE Solution in UK,” available at: http://www.airspan.com/2012/02/23/virgin-media-trials-airspan%E2%80%99s-small-cell-lte-solution-in-uk/ (accessed 31 December 2012)

[34] Press release, “Huawei Launches Wireless Backhaul Solution,” available at: http://www.huawei.com/en/about-huawei/newsroom/press-release/hw-134455-wirelessbackhaulsolutionerelay.htm (accessed 31 December 2012)

[35] Infonetics Research, “Outdoor small cell backhaul a 5-year $5 billion opportunity,” available at: http://www.infonetics.com/pr/2012/Outdoor-Small-Cell-Mobile-Backhaul-Equipment-Market-Outlook-Highlights.asp (accessed 31 December 2012)

[36] Application note, “Wireless Backhaul Solutions for Small Cells,” available at: http://www.ceragon.com/files/Ceragon%20-%20Small%20Cell%20-%20Application%20Note.pdf (accessed 31 December 2012)

II. Included papers

A On the Impact of Backhaul Channel Reliability on Cooperative Wireless Networks

To appear in the proceedings of the

2013 IEEE International Conference on Communications (ICC)

Wireless Communications Symposium,

Budapest, June 9-13, 2013.

On the Impact of Backhaul Channel Reliability on Cooperative Wireless Networks

Zoltán Mayer, Jingya Li, Agisilaos Papadogiannis, and Tommy Svensson
Department of Signals and Systems, Chalmers University of Technology, Gothenburg, Sweden
zoltanm@student.chalmers.se, {jingya.li, agisilaos.papadogiannis,tommy.svensson}@chalmers.se

Abstract—**We study the effect of unreliable backhaul links on the performance of Coordinated Multi-Point (CoMP) techniques. CoMP has emerged as a powerful scheme to mitigate co-channel interference. Economically viable deployment of Heterogeneous Networks (HetNets) will require the use of lower-performance backhaul options, e.g. non-line-of-sight (NLOS) microwave links. Motivated by HetNets, a backhauling model is introduced, by assigning Link Failure Probability (LFP) to backhaul links, for the cooperative clusters. In this paper we analyze the centralized and semi-distributed CoMP architectures. We investigate the probability of deficient backhaul links reducing quality of service, by impeding transmission. By evaluating the average sum rate of users within a CoMP cluster, we show how backhaul link reliability affects the performance of the cooperative cluster. We conclude, that the performance gains offered by CoMP quickly diminish, as the unreliability of the backhaul links grows.**

I. Introduction

Driven by the increasing popularity of connected devices in wireless communication systems, e.g., smartphones and tablets, mobile broadband traffic is growing rapidly. As cloud-based services become essential to our daily lives, users want to be connected anytime and from anywhere [1]. Traditional macrocell systems fall short to satisfy these needs. Macrocells are inadequate when providing indoor coverage due to the signal attenuation while penetrating the outer walls of the buildings [2]. More importantly, since numerous users are in the coverage area of each macrocell, any single user equipment (UE) gets only a small share of network resources, limiting throughput. To satisfy demand for mobile bandwidth while reducing cost per bit, the spectral efficiency of cellular networks needs to be significantly increased [3].

The spectral efficiency of a cellular network can be improved by increasing the cell density and reducing the transmission power of the network nodes. Hence, embedding low-power nodes into the existing networks, so as to obtain a so called heterogeneous network (HetNet), has emerged as a viable way to increase network capacity [4]. However, a major challenge of HetNets is the management of co-channel interference [5]. From information theory it is known that inter-cell interference can be overcome, if transmission nodes (TN) cooperatively process signals [6]. Recently such techniques are referred to as Coordinated Multi-Point (CoMP) [7]. CoMP schemes allow interference mitigation through joint and coherent transmission from multiple TNs, but at the cost of increased complexity and other overhead [8].

Part of this work has been performed in the framework of the FP7 project ICT-317669 METIS, which is partly funded by the EU. The authors would like to acknowledge the contributions of their colleagues in METIS, although the views expressed are those of the authors and do not necessarily represent the project. This work is also supported by the Swedish Agency for Innovation Systems (VINNOVA), within the P36604-1 MAGIC project.

CoMP requires information exchange between the TNs, in which each TN acquires the counterpart's channel state information (CSI) or user data, prior to the coordinated transmission. The information exchange occurs over the backhaul links that interconnect the TNs. Traditionally, backhaul links are assumed to be highly reliable, which are less likely to be available in the heterogeneous and dense future networks. This is because the high number of access nodes would need to be accompanied by a proportionally high financial investment in order to build high quality wireline backhaul [9]. Furthermore the topology of heterogeneous access points, i.e., some will be mounted on high towers (macro stations), others will be deployed on the street level below roof tops (pico and relay stations) and others will be indoors (femto cells), suggests that backhaul links interconnecting access nodes are wireless and without guaranteed line-of-sight (LOS) [10].

In this paper, motivated by the HetNet scenario, we evaluate the downlink of a cooperative wireless network, and study the impact of backhaul channel reliability on the system performance. A backhauling model is introduced for the cooperative systems under different network architectures, i.e., the centralized and semi-distributed versions. An analytical approach is taken to investigate how backhaul reliability affects the operation of the cooperating TNs. Under each considered network CoMP architecture, the zero-forcing joint transmission scheme and the multi-point coordinated scheduling scheme are studied and compared. We have found, that although higher rates are achievable with joint transmission, it is more sensitive to backhaul link failure. The semi-distributed architecture offers better resistance to LFP, as the performance of the CoMP schemes will converge to the one of traditional single cell transmission, as LFP grows.

The rest of the paper is organized as follows. In Section II, we present the proposed system model. In Section III, we describe the examined backhauling models for different system architectures, and Section IV illustrates how backhaul reliability affects TN operation under the described CoMP architectures. The numerical results are discussed in Section V, and the conclusions are drawn in Section VI.

Notation: Here, $(\,)^H$, $(\,)^T$, $(\,)^{-1}$ and $(\,)^+$ denote the conjugate transpose, transpose, matrix inversion and matrix pseudo-inversion operations, respectively. The notation $\mathbf{1}_{[m\times n]}$ and $\mathbf{0}_{[m\times n]}$ represent the matrix with m rows and n columns filled with ones and zeros, respectively. $(\,)^m_{(n,:)}$ denotes the n^{th} row of matrix m. $\mathbb{N}$ refers to the set of natural numbers. $|\mathcal{M}|$ denotes the cardinality of the set $\mathcal{M}$. $\odot$ represents the element-wise multiplication.

II. System Model

In this paper, we consider the downlink of a cooperative system, consisting of N single-antenna TNs and M single-antenna UEs. The UEs are grouped together using a particular resource slot. Hence, in the following, the case where $M = N$ will be assumed. The N TNs are assumed to have the same maximum power constraint $P_{\max}$ and to share the same resource slot. Let $\mathbf{x} = [x_1, ..., x_N]^T$ denote the signal vector transmitted from all N TNs, with $x_n^H x_n \leq P_{\max}$ for all $n \in \{1, ..., N\}$. The received signal at UE m can then be expressed as $y_m = \mathbf{h}_m \mathbf{x} + n_m$, where $\mathbf{h}_m = [h_{m1}, ..., h_{mN}]$ denotes the channel state vector between UE m and all N TNs. n_m is the sum of the thermal noise and the uncoordinated out-of-cluster interference, modeled as independent complex additive white Gaussian noise [11].

Each UE m estimates its channel state vector $\mathbf{h}_m$, and feeds it back to its serving TN m via uplink control channels, that are assumed to be fully reliable, since we in this work aim to investigate the impact of unreliable backhaul links. The Control Unit (CU) gathers CSI from the cooperating TNs via backhaul links and designs the transmission parameters [12]. It is assumed that the CSI of all UEs within the system, named as full CSI, is corrupted via backhaul channels. Hence, the system channel matrix available at the CU is denoted as $\hat{\mathbf{H}} = [\hat{\mathbf{h}}_1^T, .., \hat{\mathbf{h}}_M^T]^T \in \mathcal{C}^{M \times N}$, which will be used for the scheduling and transmission scheme design.

A. Joint Transmission

Assume that the data symbols of all the M UEs within the cluster are shared among the N coordinated TNs. A linear precoding approach, zero-forcing, is considered as the coherent joint transmission scheme in this section. Note that with linear precoding among N single-antenna TNs, at most N single-antenna UEs can be served on the same resource slot without inter-user interference.

Let $\mathcal{M}$ denote the set of scheduled UEs in a given resource slot, with $\mathcal{M} \subseteq \{1, ..., M\}$ and $|\mathcal{M}| \leq N$. Let $\mathbf{b} \in \mathbb{C}^{|\mathcal{M}|}$ be the data symbols of the selected UEs in set $\mathcal{M}$. A precoding matrix $\mathbf{W} = [\mathbf{w}_1, ..., \mathbf{w}_{|\mathcal{M}|}] \in \mathcal{C}^{N \times |\mathcal{M}|}$ is designed for mapping the data symbol vector $\mathbf{b}$ into the transmit signal vector $\mathbf{x}$, that is, $\mathbf{x} = \mathbf{W}\mathbf{b}$. The m^{th} column of $\mathbf{W}$, $\mathbf{w}_m = [w_{1m}, ..., w_{Nm}]^T$, is the precoding vector for UE m in the set $\mathcal{M}$. The received signal of UE m can be rewritten as $y_m = \mathbf{h}_m \mathbf{w}_m b_m + \sum_{i \in \mathcal{M}, i \neq m} \mathbf{h}_m \mathbf{w}_i b_i + n_m$.

Let $p_m = b_m b_m^H$ denote the symbol power allocated to UE m across the N TNs. The signal to interference plus noise ratio (SINR) of UE m is then given by

$$\gamma_m = \frac{\|\mathbf{h}_m \mathbf{w}_m\|^2 p_m}{\sum_{i \in \mathcal{M}, i \neq m} \|\mathbf{h}_m \mathbf{w}_i\|^2 p_i + \sigma^2}. \quad (1)$$

Thus, the sum rate of the cluster can be expressed as

$$C = \sum_{m \in \mathcal{M}} \log_2(1 + \gamma_m). \quad (2)$$

Using zero-forcing precoding, the precoding matrix, $\mathbf{W}$, is obtained as the pseudo-inverse of the channel matrix, $\hat{\mathbf{H}}$, available at the CU.

In order to reduce the complexity, a sub-optimal equal power allocation is considered [13]. As a first step, $\mathbf{W}$ is normalized column-wise, then for any given UE set, $\mathcal{M}$, the power allocation vector is derived as

$$\mathbf{p} = \left\{ \min_{n=1,...N} \frac{P_{\max}}{\sum_{m \in \mathcal{M}} \|w_{nm}\|^2} \right\} \mathbf{1}_{[|\mathcal{M}| \times 1]}. \quad (3)$$

By solving the joint power allocation of (3) for every possible UE set $\mathcal{M}$, the chosen UE set $\mathcal{M}^{\text{JT}}$ and $\mathbf{p}^{\text{JT}}$ will be the ones that achieve the highest $\sum_{m=1}^{M} \log_2(1 + \hat{\gamma}_m)$, where $\hat{\gamma}_m$ is derived from (1) by using the obtained $\hat{\mathbf{h}}_m$ at the CU instead of the true channel vector $\mathbf{h}_m$. In the following, this zero-forcing joint transmission scheme is denoted as JT.

B. Coordinated Scheduling

In the considered coordinated scheduling scheme, data to a single UE is only transmitted from its serving TN, which is selected based on the long term channel quality measurements, including pathloss and shadow fading. Hence, user data exchange between TNs is not needed. It is assumed that a TN can transmit data to at most one UE in any given resource slot.

Let $P_m = b_m^H b_m$ denote the transmit power of TN m to UE m, with $P_m \leq P_{\max}$. Then, the SINR for UE m is given as

$$\gamma_m = \frac{\|h_{mm}\|^2 P_m}{\sum_{j=1, j \neq m}^{j=N} \|h_{mj}\|^2 P_j + \sigma^2}. \quad (4)$$

Thus, the sum rate can be calculated by (2).

UE scheduling and power allocation decisions are jointly made at the CU to control ICI. With the gathered channel matrix, $\hat{\mathbf{H}}$, the CU designs the UE selection indicator matrix $\mathbf{S}$ and the power allocation vector $\mathbf{P} = [P_1, ..., P_n]$, in order to maximize the sum rate subject to per-TN power constraints. Based on [14], a suboptimal binary power control (BPC) is considered for this coordinated scheduling scheme, i.e., $P_n = 0$ or $P_{\max}$ for $\forall n \in \{1, ..., N\}$. Then, the relaxed problem becomes an exhaustive binary search. The CU searches all feasible boundary point sets, i.e., $P_n = 0$ or $P_{\max}$ for $\forall n \in \{1, ..., N\}$. The chosen transmit power vector $\mathbf{P}^{\text{CS}}$ will be the ones that achieve the highest $\sum_{m=1}^{M} \log_2(1 + \hat{\gamma}_m)$, where $\hat{\gamma}_m$ is derived from (4) by using the obtained $\hat{\mathbf{h}}_m$. In this paper, this scheme is named as CS.

III. Backhauling Models

In this section, we introduce the backhauling models considered for single cell transmission and for the cooperative systems under different network architectures, i.e., the centralized and semi-distributed CoMP architectures.

A. Single Cell Transmission

Single cell transmission without TN coordination (Fig. 1), denoted as SC, is used as a baseline. For SC transmission, the data blocks sent from the core network to TN n will only contain the data symbol for UE n. The TNs might fail in decoding the received data blocks, due to backhaul unreliability. This event is modeled by erasing each data symbol, b_n, independently. There is no cooperation, therefore CSI is not to be shared, hence backhaul unreliability only affects the data distribution.

B. Centralized CoMP Architecture

As depicted in Fig. 2, under the centralized architecture each TN n forwards their received local channel state row vector, $\mathbf{h}_m$, to the CU via backhaul links in a first step. Based on the gathered system channel matrix $\hat{\mathbf{H}}$, the CU constructs the precoding matrix for the JT scheme or makes scheduling decisions for the CS scheme. Once the decisions are made, the CU forwards them via backhaul links to each coordinated TN. Hence, backhaul links are used twice, i.e., gathering full CSI and distributing transmission decisions.

All backhaul links are modeled to be prone to errors, leading to losing partial CSI of the system at the CU or losing precoded user data at the cooperating TNs. LFPs are modeled as independent binary discrete random variables. Hence the available system channel matrix at CU, $\hat{\mathbf{H}}$, is obtained as

$$\hat{\mathbf{H}} = \mathbf{H} \odot \mathbf{H}^{\text{mask}}, \tag{5}$$

where $\mathbf{H}$ is the true system channel matrix. Here, $\mathbf{H}^{\text{mask}}$ is a binary mask matrix, where each row vector, $\mathbf{H}^{\text{mask}}_{(m,:)}$, is either $\mathbf{0}_{[1\times N]}$ with probability $P^{\text{C}}_{\text{F}_n}$ or $\mathbf{1}_{[1\times N]}$.

For the JT scheme, the user data x_n distributed from the CU to TN n contains the precoded data symbols for the scheduled UEs, i.e., $x_n = \mathbf{W}_{(n,:)}\mathbf{b} = \sum_{m\in\mathcal{M}} w_{nm} b_m$.

Similarly, to model the data loss via backhaul links to each TN, a binary mask matrix, $\mathbf{W}^{\text{mask}}$, is applied to the original precoding matrix $\mathbf{W}$ as

$$\hat{\mathbf{W}} = \mathbf{W} \odot \mathbf{W}^{\text{mask}}, \tag{6}$$

which erases each row vector of $\mathbf{W}$ independently, with a probability of $P^{\text{D}}_{\text{F}_n}$. The SINR of the scheduled UEs can be derived by substituting $\hat{\mathbf{W}}$ into (1), the sum rate can then be obtained from (2).

Example 1. A cooperative cluster comprises of $N = 3$ TNs, as shown in Fig. 2. All UEs feed back the local channel state vector to their serving TN. TNs share the received local channel state vector, $\mathbf{h}_m$, with the CU. If, however, $\mathbf{h}_2$ is lost due to failure of the backhaul link, $\hat{\mathbf{H}}$ is obtained as

$$\hat{\mathbf{H}} = \begin{bmatrix} \mathbf{h}_1 \\ \mathbf{h}_2 \\ \mathbf{h}_3 \end{bmatrix} \odot \begin{bmatrix} 1 & 1 & 1 \\ 0 & 0 & 0 \\ 1 & 1 & 1 \end{bmatrix}.$$

Considering an error in the backhaul link when the CU distributes the precoded user data to TN 1, $\hat{\mathbf{W}}$ is calculated as

$$\hat{\mathbf{W}} = \mathbf{W} \odot \begin{bmatrix} 0 & 0 & 0 \\ 1 & 1 & 1 \\ 1 & 1 & 1 \end{bmatrix}.$$

For the CS scheme, the user data distributed from the CU is $x_n = z_n b_n$, where z_n is the discrete binary power control bit.

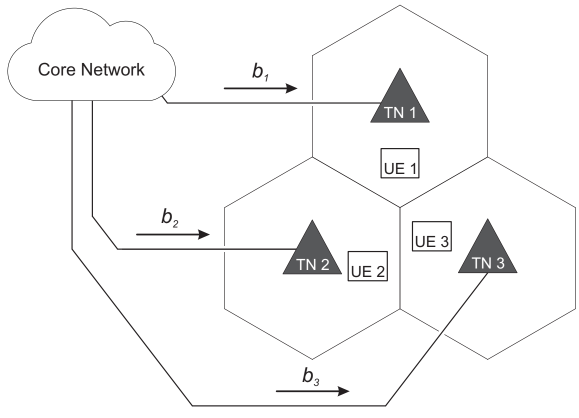

Figure 1. Single cell transmission

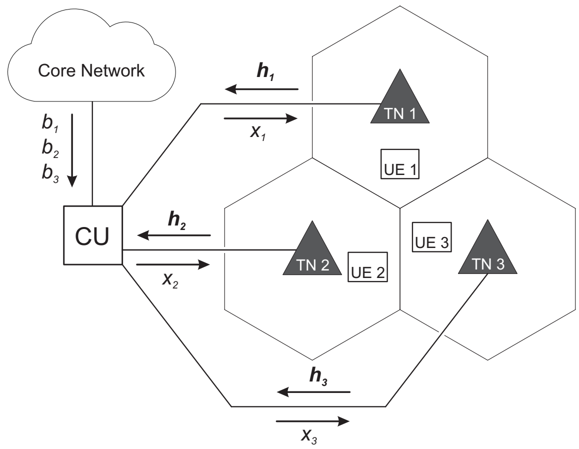

Figure 2. Centralized CoMP architecture

In this case, the data loss due to backhaul unreliability is modeled as

$$\hat{b}_n = b_n b^{\text{mask}}_n, \tag{7}$$

where b^{mask}_n is a binary mask variable which erases the data symbol of UE n with probability $P^{\text{D}}_{\text{F}_n}$. Thus, the SINR of each UE n can be calculated by substituting $\mathbf{P}^{\text{mask}}$ into (4), where the n^{th} element, P^{mask}_n, is derived by $P^{\text{mask}}_n = b^{\text{mask}}_n P^{\text{CS}}_n$.

C. Semi-distributed CoMP Architecture

Under the semi-distributed architecture, depicted in Fig. 3, the received local CSI vectors $\mathbf{h}_m$ are firstly shared between TNs via interconnecting backhaul links. Each TN receives $N-1$ non-local CSI vectors, thus acquiring a local gathered system channel matrix $\hat{\mathbf{H}}_n$, which is obtained independently by using (5). Note that we assume that every TN n receives an error-free local CSI vector, $\mathbf{h}_m$, fed back by UE m in each resource slot. Here $M = N$, hence, the m^{th} row of $\mathbf{H}^{\text{mask}}$ will always be $\mathbf{1}_{[1\times N]}$.

Based on the gathered $\hat{\mathbf{H}}_n$, each cooperating TN acts as a CU, independently designing its own precoding weights and power allocation vector for JT, or make scheduling decisions for CS. Transmission decisions are then locally applied to the user data, which is assumed to be received from the core network.

For the JT scheme, each TN n independently designs the precoding matrix $\mathbf{W}^n$ based on the gathered system matrix $\hat{\mathbf{H}}_n$. The n^{th} row of $\mathbf{W}^n$, i.e., $W^n_{(n,:)}$, is then chosen by TN n as the precoding vector for mapping the user data symbols into the transmit signal. The data blocks, sent from the core network to TN n, will contain all data symbols for the scheduled UEs in the cluster, $d_n = [b_1, ..., b_m]$. We assume that different user data symbols are sent from the core network to all TNs independently via backhaul links. Thus, each user data symbol, b_m, is affected independently by backhaul link failure. To model this LFP a binary mask is applied to $\mathbf{W}$, similarly to (6). In this case, all elements of $\mathbf{W}^{\text{mask}}$ will be independently ones or zeros. Finally the SINR of the scheduled UEs can then be derived by substituting $\hat{\mathbf{W}}$ into (1), and the sum rate can then be obtained from (2).

Example 2. A cooperative cluster comprises of $N = 3$ TNs, as shown in Fig. 3. All UEs feed back the local channel state vector to their serving TN. TN 1 receives the error-free channel state vector $\mathbf{h}_1$ from UE 1. TN 2 and TN 3 share $\mathbf{h}_2$ and $\mathbf{h}_3$ with TN 1 through unreliable backhaul links. Considering the case when $\mathbf{h}_3$ is lost due to failure of the backhaul link, $\hat{\mathbf{H}}_1$ is obtained as

$$\hat{\mathbf{H}}_1 = \begin{bmatrix} \mathbf{h}_1 \\ \mathbf{h}_2 \\ \mathbf{h}_3 \end{bmatrix} \odot \begin{bmatrix} 1 & 1 & 1 \\ 1 & 1 & 1 \\ 0 & 0 & 0 \end{bmatrix} .$$

The data symbols from the core network are affected by errors independently, therefore, $\hat{\mathbf{W}}$ is derived as shown in the example below:

$$\hat{\mathbf{W}} = \begin{bmatrix} W^1_{(1,:)} \\ W^2_{(2,:)} \\ W^3_{(3,:)} \end{bmatrix} \odot \begin{bmatrix} 1 & 1 & 0 \\ 0 & 1 & 0 \\ 1 & 0 & 1 \end{bmatrix} .$$

For the CS scheme, the downlink data block, d_n, which is distributed from the core network to each TN n, contains only the data symbol of its own UE. Thus, $d_n = b_m$, with $n = m$. The discrete binary power control bit z_n is designed locally at each TN. Modeling backhaul unreliability and calculation of the SINR can be done in the same way as described above for the centralized architecture.

IV. Backhaul Reliability Analysis

In this section we analyze the probability of any TN n staying silent in a resource slot, P^{S}_n, due to unreliable backhaul links. This may cause some UEs unserved, or, as a worst-case scenario, impede all transmission with probability $P^{\text{W}} = \prod_{n=1}^{N} P^{\text{S}}_n$.

A. Single Cell Transmission

No CSI sharing takes place, therefore transmission only depends on the LFP of the backhaul links connecting the TNs to the network. Provided that the LFP of the backhaul link is P_{F_n}, P^{S}_n can be expressed as

$$P^{\text{S}}_n = P_{\text{F}_n} . \tag{8}$$

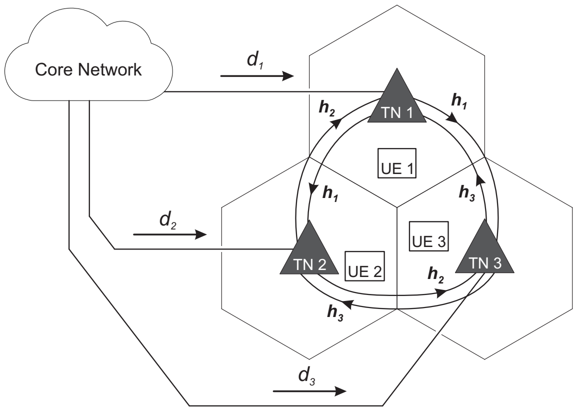

Figure 3. Semi-distributed CoMP architecture

B. Centralized CoMP architecture

Joint Transmission: Considering the JT scheme under the centralized architecture, based on the backhauling model described in Section III, TN n will stay silent if

Case 1. All local CSI vectors sent from the TNs are lost at the CU, otherwise,

Case 2. The user data distributed from the CU to TN n is lost.

The probability that Case 1 happens is $\prod_{i=1}^{N} P^{\text{C}}_{\text{F}_i}$, where $P^{\text{C}}_{\text{F}_n}$ is the LFP when TN n forwards the CSI to the CU. Case 2 happens with probability $P^{\text{D}}_{\text{F}_n}$, where $P^{\text{D}}_{\text{F}_n}$ is the LFP when the CU distributes precoded user data to TN n. Therefore, P^{S}_n for the JT scheme under centralized architecture can be expressed as

$$P^{\text{S}}_n = P^{\text{D}}_{\text{F}_n} + (1 - P^{\text{D}}_{\text{F}_n}) \cdot \prod_{i=1}^{N} P^{\text{C}}_{\text{F}_i} . \tag{9}$$

Coordinated Scheduling: In case of the CS scheme, it is possible that the TN will not be scheduled for transmission in the current resource block even if CSI sharing is not affected by failure of backhaul links, because BPC is performed to control the interference, depending on the system architecture and the current channel conditions. Hence, TN n will stay silent if

Case 1. The TN will not be scheduled for transmission in the current resource block, due to BPC, otherwise,

Case 2. The user data distributed from the CU to TN n is lost.

The probability that Case 1 happens is P^{NS}_n, while Case 2 happens with probability $P^{\text{D}}_{\text{F}_n}$. Therefore, P^{S}_n for the CS scheme under centralized architecture can be expressed as

$$P^{\text{S}}_n = P^{\text{D}}_{\text{F}_n} + (1 - P^{\text{D}}_{\text{F}_n}) \cdot P^{\text{NS}}_n . \tag{10}$$

C. Semi-distributed CoMP architecture

Joint Transmission: In case of the JT scheme P^{S}_n depends on whether CSI from other TNs has reached TN n, and whether the user data has reached the TN in question. Hence, TN n will stay silent if

Case 1. All non-local CSI vectors, sent from other TNs, and the data symbol of UE n, sent from the core network, are lost at TN n, otherwise,

Case 2. All user data symbols distributed from the core network to TN n are lost.

The probability that Case 1 happens is $P^{\mathrm{D}}_{\mathrm{F}_{n,n}} \cdot \prod_{k=1,k\neq n}^{N} P_{\mathrm{F}_{n,k}}$. $P^{\mathrm{D}}_{\mathrm{F}_{m,n}}$ is the LFP between the core network and TN n, while user data symbol m is distributed. $P_{\mathrm{F}_{n,k}}$ is the LFP when CSI is sent from TN k to TN n. Case 2 happens with probability $\prod_{m=1}^{M} P^{\mathrm{D}}_{\mathrm{F}_{m,n}}$. Transmission from TN n to a UE m, if $m \neq n$, will happen with probability $\left(1 - P^{\mathrm{D}}_{\mathrm{F}_{m,n}}\right) \cdot \left(1 - P_{\mathrm{F}_{n,m}}\right) = 1 - \left[P^{\mathrm{D}}_{\mathrm{F}_{m,n}} + \left(1 - P^{\mathrm{D}}_{\mathrm{F}_{m,n}}\right) \cdot P_{\mathrm{F}_{n,m}}\right]$. Therefore, P^{S}_{n} for the JT scheme under semi-distributed architecture can be expressed as

$$P^{\mathrm{S}}_{n} = P^{\mathrm{D}}_{\mathrm{F}_{n,n}} \cdot \prod_{i\in T} \left[P^{\mathrm{D}}_{\mathrm{F}_{n,i}} + \left(1 - P^{\mathrm{D}}_{\mathrm{F}_{n,i}}\right) \cdot P_{\mathrm{F}_{n,i}}\right], \qquad (11)$$

where $T = \{x \in \mathbb{N} : 1 \leq x \leq N,\ x \neq n\}$.

Coordinated Scheduling: Considering the CS scheme under the semi-distributed architecture, P^{S}_{n} can be calculated using (10). In this case, however, P^{NS}_{n} will depend on the reliability of the backhaul links interconnecting the TNs, and $P^{\mathrm{D}}_{\mathrm{F}_{n}}$ models LFP between the core network and TN n.

V. Performance Evaluation

We consider the downlink of a CoMP cluster with $N = 2$ and $N = 3$ neighboring sectors respectively. For each cluster size, N, $M = N$ single-antenna UEs are grouped together using a particular resource slot.[1] The cluster radius R is 500 m. The path loss model is $PL(d) = 128.1 + 37.6 \log_{10}(d)$ in dB, with d given in km. Shadowing is log-normally distributed with zero mean and standard deviation 8 dB. The system SNR is set to 18 dB, which is defined as the received SNR at the boundary of the cell, assuming full power transmission $P_{\max}$ from the TN, accounting only for pathloss $PL(R)$ and ignoring shadowing and fast fading [15]. For each value of LFP, the average sum rate, $\overline{C}$, is obtained by averaging the sum rate of the cluster, obtained from (2), over $2 \cdot 10^5$ independent UE set realizations.

UEs are uniformly distributed over the cell area. Each TN has a single UE allocated in the shared frequency, time-slot or code resource. SC transmission without TN coordination, denoted as Single Cell, is used as baseline. For each of the analyzed CoMP architectures, i.e., the centralized and semi-distributed versions, the considered JT, CS, and SC transmission schemes are evaluated and compared. For the sake of simplicity, it is assumed that all backhaul links have the same LFP, P_{F}.

Fig. 4*a* and Fig. 4*b* plot $\overline{C}$ against LFP. If LFP is close to zero the coordinated transmission schemes offer a significant performance gain under both the centralized and semi-distributed CoMP architectures. However, this gain diminishes quickly as backhaul unreliability grows. Note that when $N = 2$, the performance of the JT scheme under the semi-distributed architecture always outperforms the one achieved under the centralized architecture. However, if $N > 2$, the centralized version outperforms the semi-distributed one for the JT scheme when the LFP is low. Moreover, within the distributed architecture, $\overline{C}$ of both JT and CS schemes converge to the performance achieved by SC transmission when the backhaul is highly unreliable. This is because, as mentioned in Section III-C, the TNs will always have at least one received local CSI vector $\mathbf{h}_m$. This causes the TNs operate similarly to the SC transmission scheme, where the performance is limited only by the reliability of the backhaul links transmitting data symbols to the TNs.

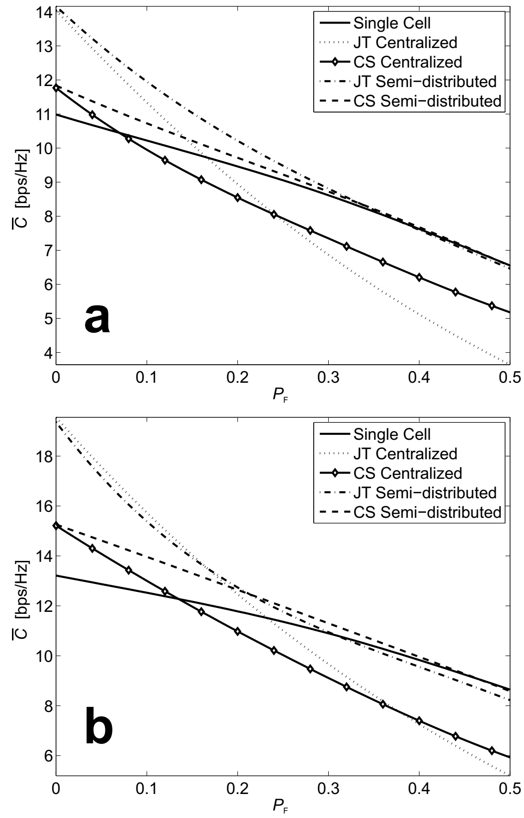

Figure 4. $\overline{C}$ vs. LFP, *a)* Cluster size = 2, *b)* Cluster size = 3

In case of the JT scheme under the centralized architecture, the CU distributes the precoded symbols in one data block towards each TN. Therefore, the data symbols of all UEs will be lost at a TN if a packet is affected by failure of the backhaul link, and this results in bad performance when LFP is high. In case of CS, if LFP is high, it is more likely that only a reduced set of TNs will be scheduled, this however increases the chance of all TNs staying silent, since the data symbols distributed for the scheduled TNs can be lost. It should be pointed out that although the semi-distributed architecture offers better performance in most cases, it requires each cooperating TN to be acting as a CU, and also backhaul links interconnecting all TNs.

We can also see that there is a cross point for JT under different architectures. As the cluster size increases the relative

[1]Note that based on the system model, $M = N$ is already a full load scenario when focusing on one resource slot.

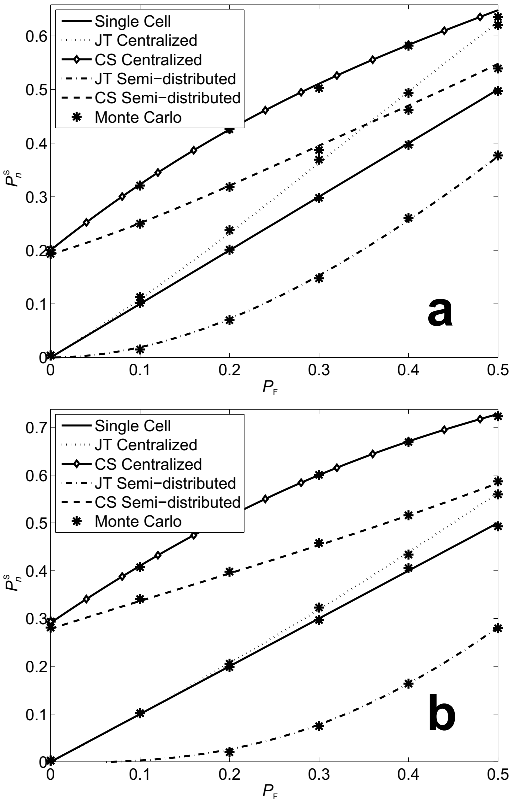

Figure 5. P_n^{S} vs. LFP, *a)* Cluster size = 2, *b)* Cluster size = 3

performance of JT under centralized architecture improves, however, it drops faster in the high LFP domain. In the evaluated scenarios the best performance can be achieved with JT under the semi-distributed architecture, however, this scheme has a higher backhaul capacity requirement, since all data symbols have to be shared with all TNs.

Fig. 5a and Fig. 5b plot the probability of any TN n staying silent in a resource slot against LFP, for each transmission scheme and system architecture. If all backhaul links have the same same LFP, P_{F}, (9)-(11) are reduced to

$$P_n^{\mathrm{S}} = P_{\mathrm{F}} + (1 - P_{\mathrm{F}}) \cdot (P_{\mathrm{F}})^N \ , \tag{12}$$

for JT under the centralized architecture,

$$P_n^{\mathrm{S}} = P_{\mathrm{F}} + (1 - P_{\mathrm{F}}) \cdot P_n^{\mathrm{NS}} \, , \tag{13}$$

for CS under both introduced architectures, and

$$P_n^{\mathrm{S}} = P_{\mathrm{F}} \cdot [P_{\mathrm{F}} + (1 - P_{\mathrm{F}}) \cdot P_{\mathrm{F}}]^{N-1} \ , \tag{14}$$

for JT under the semi-distributed architecture.

The simulated data is plotted with markers only, while the continuous lines show the values calculated by (12)-(14). Note, that P^{S} does not directly limit $\overline{C}$, since the silence of a TN also decreases the inter-cell interference in the neighboring cells.

VI. Conclusions

In this paper we have examined the effects of backhaul reliability on the performance of a cluster of cooperative transmission nodes. In particular, two transmission schemes, joint transmission and coordinated scheduling were evaluated under the centralized and semi-distributed CoMP architectures. The scenarios were assessed in terms of average sum rate in the coverage region, and traditional single cell transmission served as a baseline for comparison. Analytical results were presented to show how unreliable backhaul degrades quality of service, by leaving some user equipments unserved.

Numerical results show that cooperative transmission techniques have the potential to greatly reduce harmful interference, therefore, increasing the system sum rate. However, the performance of the system highly depends on the reliability of the backhaul network. Although all examined scenarios suffer from performance degradation as LFP increases, the coordinated scheduling scheme always shows a better performance under the semi-distributed architecture. For the joint transmission scheme, if the number of cooperating transmission nodes is greater than two, better system performance can be achieved under the centralized architecture, but only up to a certain value of LFP, which is determined by the cluster size.

References

[1] D. McQueen, "The momentum behind LTE adoption," *IEEE Commun. Mag.*, vol. 47, no. 2, pp. 44–45, Feb. 2009.

[2] C. Gandarillas, V. Iglesias, M. Aparicio, E. Mino-Díaz, P. Olmos, "A new approach for improving indoor LTE coverage," *IEEE GLOBECOM Workshops 2011*, pp. 1330 – 1335, Dec. 2011.

[3] V. Chandrasekhar, J. G. Andrews and A. Gatherer, "Femtocells Networks: A Survey," *IEEE Commun. Mag.*, vol. 46, no. 9, pp. 59–67, Jun. 2008.

[4] A. Ghosh, J. G. Andrews, N. Mangalvedhe, R. Ratasuk, B. Mondal, M. Cudak, E. Visotsky, T. A. Thomas, P. Xia, H. S. Jo, H. S. Dhillon, T. D. Novlan, "Heterogeneous Cellular Networks: From Theory to Practice", *IEEE Commun. Mag.,* vol. 50, no. 6, pp. 54–64, Jun. 2012.

[5] G. Boudreau, J. Panicker, N. Guo, R. Chang, N. Wang, and S. Vrzic, "Interference Coordination and Cancellation for 4G Networks," *IEEE Commun. Mag.*, vol. 47, no. 4, pp. 74–81, Apr. 2009.

[6] A. Barbieri, P. Gaal, S. Geirhofer, T. Ji, D. Malladi, Y. Wei, F. Xue, "Coordinated downlink multi-point communications in heterogeneous cellular networks," in *IEEE ITA 2012*, San Diego, CA, Feb. 2012.

[7] Y. H. Nam, L. J. Liu, Y. Wang, C. Zhang, J. Cho and J. K. Han, "Cooperative communication technologies for LTE-Advanced" *IEEE ICASSP 2010*, pp. 5610–5613, Mar. 2010.

[8] F. Pantisano, M. Bennis, W. Saad, M. Debbah, M, Latva-aho, "On the Impact of Heterogeneous Backhauls on Coordinated Multipoint Transmission in Femtocell Networks," in *IEEE ICC 2012*, Ottawa, Canada, Jun. 2012.

[9] O. Tipmongkolsilp, S. Zaghloul, A. Jukan, "The evolution of cellular backhaul technologies: Current issues and future trends," *IEEE Commun. Surveys Tut.*, vol. 13, no. 1, pp. 97–113, 1st Quart., 2011.

[10] M. Coldrey, H. Koorapaty, J.-E. Berg, Z. Ghebretensaé, J. Hansryd, A. Derneryd, S. Falahati, "Small-Cell Wireless Backhauling," in *IEEE VTC 2012*, Québec City, Canada, Sep. 2012.

[11] J. Li, A. Papadogiannis, R. Apelfröjd, T. Svensson, and M. Sternad, "Performance Evaluation of Coordinated Multi-Point Transmission Schemes with Predicted CSI," in *IEEE PIMRC 2012*, Sydney, Australia, Sep. 2012.

[12] A. Papadogiannis, E. Hardouin, and D. Gesbert, "Decentralising multicell cooperative processing: A novel robust framework," *EURASIP J. Wireless Commun. Netw.*, vol. 2009, p. 10, Aug. 2009.

[13] A. Papadogiannis, H. J. Bang, D. Gesbert and E. Hardouin, "Efficient selective feedback design for multicell cooperative networks," *IEEE Trans. Vehicular Techn.*, vol. 60, no. 1, pp. 196–205, Jan. 2011.

[14] A. Gjendemsjø, D. Gesbert, G. Øien and S. Kiani, "Binary power control for sum rate maximization over multiple interfering links," *IEEE Trans. Wireless Commun.*, vol. 7, no. 8, pp. 3164–3173, Aug. 2008.

[15] 3GPP TR 36.814 v9.0.0, "Evolved Universal Terrestrial Radio Access (E-UTRA); Further advancement of E-UTRA physical layer aspects (Release 9)," Mar. 2010.

B On the Impact of Control Channel Reliability on Coordinated Multi-Point Transmission

Submitted to

European Association for Signal Processing (EURASIP)

Journal on Wireless Communications and Networking

On the Impact of Control Channel Reliability on Coordinated Multi-Point Transmission

Zoltán Mayer, Jingya Li, Agisilaos Papadogiannis, and Tommy Svensson

Abstract

In the heterogeneous networks (HetNets), co-channel interference is a serious problem. Coordinated multi-point (CoMP) transmission has emerged as a powerful technique to mitigate co-channel interference. However, all CoMP techniques rely on information exchange through reliable control channels, which are unlikely to be available in HetNets. In this paper, we study the effect of unreliable control channels, consisting of the access links and backhaul links, on the performance of CoMP. A control channel model is introduced by assigning link failure probability (LFP) to backhaul and access links for the cooperative clusters. Three CoMP architectures, namely the centralized, semi-distributed and fully distributed are analyzed. We investigate the probability of deficient control channels reducing quality of service, and impeding transmission. General closed-form expressions are derived for the probability of a cooperative transmission node staying silent in a resource slot due to unreliable control links. By evaluating the average sum rate of users within a CoMP cluster, we show that the performance gains offered by CoMP quickly diminish, as the unreliability of the control links grows.

Index Terms

Coordinated multi-point (CoMP), heterogeneous networks (HetNet), backhaul reliability, control channel, link failure probability

Z. Mayer, J. Li, A. Papadogiannis and T. Svensson are with the department of Signals and Systems, Chalmers University of Technology, Gothenburg, Sweden. (email: zoltanm@student.chalmers.se, {jingya.li, agisilaos.papadogiannis, tommy.svensson}@chalmers.se).

I. INTRODUCTION

Driven by the increasing popularity of connected devices in wireless communication systems, e.g., smartphones and tablets, mobile broadband traffic is growing rapidly. As cloud-based services become essential to our daily lives, users want to be connected anytime and from anywhere [1]. Traditional macrocell systems fall short to satisfy these needs, partly because increasing the available frequency spectrum is not an option, due to the fact that bandwidth is an extremely expensive and increasingly scarce commodity which is severely regulated. Macrocells can be also inadequate in providing indoor coverage due to the signal attenuation while penetrating the outer walls of the buildings [2]. More importantly, since numerous users are in the coverage area of each macrocell, any single user equipment (UE) gets only a small share of network resources, limiting throughput. To satisfy demand for high data rates while reducing cost per bit, the spectral efficiency of cellular networks needs to be significantly increased [3].

The spectral efficiency of a cellular network can be improved by increasing the cell density and reducing the transmission power of the network nodes. Hence, embedding low-power nodes into the existing networks, so as to form a heterogeneous network (HetNet), has emerged as a viable way to increase network capacity [4]. Short-range, plug-and-play indoor base stations promise to boost achievable throughput and fill the coverage holes. However, a major challenge of HetNets is the management of co-channel interference [5]. From information theory it is known that inter-cell interference can be overcome, if transmission nodes (TN) process signals in a cooperative manner [6]. Recently such techniques are referred to as coordinated multi-point (CoMP) [7]- [9]. CoMP schemes allow interference mitigation through joint and coherent transmission from multiple TNs, but at the cost of increased complexity and signaling overhead [10]- [12].

In spite of the significant performance gain that CoMP can provide, the use of CoMP in real systems results in a substantial control signaling overhead. The control signaling information includes the channel state information (CSI) sent over the access links between TNs and users, as well as the user scheduling and transition decisions sent over backhaul links between different TNs. In this paper, these access links and backhaul links are named as control channels. The effects of control channel constraints have been studied for downlink UTRAN LTE, MIMO transmission schemes and relay node selection. As shown in [13]- [16], unreliable control channels can greatly degrade the overall network performance.

The efficiency of all CoMP schemes rely heavily on the properties of the control channels. Traditionally, backhaul links are assumed to be highly reliable, which are less likely to be available in the heterogeneous and future dense networks. This is because the high number of access nodes would need to be accompanied by a proportionally high financial investment in order to build high quality wireline backhaul [17]. Furthermore, the topology of heterogeneous access points, i.e., some will be mounted on high towers (macro stations), others will be deployed on the street level below roof tops (pico and relay stations) and others will be indoors (femto cells), suggests that backhaul links interconnecting access nodes are wireless and without guaranteed line-of-sight (LOS) [18].

This paper aims to extend and further develop the work originally reported by the authors in [19]. Motivated by the HetNet scenario, we evaluate the downlink of a cooperative wireless network, and study the impact of control channel reliability on the system performance with different CoMP techniques. A control channel model is introduced for the cooperative systems under different network architectures, i.e., the centralized, semi- and fully distributed versions. An analytical approach is taken to investigate how backhaul and access link reliability affects the operation of the cooperating TNs. We provide general closed-form expressions to assess the probability of a TN staying silent in a resource slot, depending on the link failure probabilities (LFP) of the backhaul network and the access links. Under each considered network CoMP architecture, the zero-forcing coherent joint transmission scheme and the multi-point coordinated scheduling scheme are studied and compared. We have found that although higher rates are achievable with both coordinated scheduling and coherent joint transmission, both schemes are very sensitive to control channel reliability. The semi- and fully distributed architectures are more robust to LFP, as the performance of the CoMP schemes under these architectures will converge to traditional single cell transmission, as LFP grows.

The rest of the paper is organized as follows. In Section II, we present the signal and system model. In Section III, the examined control channel models for different system architectures are introduced. Section IV illustrates how backhaul and access link reliability affects TN operation under the described CoMP architectures. The numerical results are discussed in Section V, and the conclusions are drawn in Section VI.

Notation: Here, $(\,)^H$, $(\,)^T$, $(\,)^{-1}$ and $(\,)^+$ denote the conjugate transpose, transpose, matrix inversion and matrix pseudo-inversion operations, respectively. The notation $\mathbf{1}_{[m\times n]}$ and $\mathbf{0}_{[m\times n]}$ represent the matrix with m rows and n columns filled with ones and zeros, respectively. $\mathbf{X}(n,:)$ denotes the n^{th} row of matrix $\mathbf{X}$. $\mathbb{N}$ refers to the set of natural numbers. $|\mathcal{M}|$ denotes the cardinality of the set $\mathcal{M}$. $\odot$ represents the element-wise multiplication.

II. Signal and System Model

In this paper, we consider the downlink of a cooperative system, consisting of N single-antenna TNs and M single-antenna UEs. The UEs are grouped together using a particular resource slot. In the following, we assume $M = N$ and the serving TN of UE $m = n$ is TN n. The N TNs are assumed to have the same maximum power constraint $P_{\max}$ and to share the same resource slot. Let $\mathbf{x} = [x_1, ..., x_N]^T$ denote the signal vector transmitted from all N TNs, with $x_n^H x_n \leq P_{\max}$ for all $n \in \{1, ..., N\}$. The received signal at UE m can then be expressed as

$$y_m = \mathbf{h}_m \mathbf{x} + n_m \,, \tag{1}$$

where $\mathbf{h}_m = [h_{m1}, ..., h_{mN}]$ denotes the channel state vector between UE m and all N TNs. Here, n_m is the sum of the thermal noise and the uncoordinated out-of-cluster interference, modeled as independent complex additive white Gaussian noise [20].

Each UE m estimates its channel state vector $\mathbf{h}_m$, and feeds it back to its serving TN m via the access link. We assume that the UEs use orthogonal resource slots during CSI feedback, therefore, the outage probability of these uplink control channels can be evaluated in terms of the minimum signal to noise ratio, ρ_0, that is required for successful transmission. The Control Unit (CU) gathers CSI from the cooperating TNs via backhaul links and designs the transmission parameters [21]. It is assumed that the CSI of all UEs within the system, named as full CSI, is corrupted via control channels, i.e. the backhaul and access links. Hence, the system channel matrix available at the CU is denoted as $\hat{\mathbf{H}} =[\hat{\mathbf{h}}_1^T, .., \hat{\mathbf{h}}_M^T]^T \in \mathcal{C}^{M\times N}$, which will be used for the scheduling and transmission scheme design.

A. Coherent Joint Transmission

Assume that the data symbols of all the M UEs within the cluster are shared among the N coordinated TNs. A linear precoding approach, zero-forcing, is considered as the coherent joint transmission scheme in this section. Note that with linear precoding among N single-antenna TNs, at most N single-antenna UEs can be served on the same resource slot without inter-user interference.

Let $\mathcal{M}$ denote the set of scheduled UEs in a given resource slot, with $\mathcal{M} \subseteq \{1, ..., M\}$ and $|\mathcal{M}| \leq N$. Let $\mathbf{b} \in \mathbb{C}^{|\mathcal{M}|}$ be the data symbols of the selected UEs in set $\mathcal{M}$. A precoding matrix $\mathbf{W} =[\mathbf{w}_1, ..., \mathbf{w}_{|\mathcal{M}|}] \in \mathcal{C}^{N\times|\mathcal{M}|}$ is designed for mapping the data symbol vector $\mathbf{b}$ into the transmit signal vector $\mathbf{x}$, that is,

$$\mathbf{x} = \mathbf{W}\mathbf{b}. \tag{2}$$

The m^{th} column of $\mathbf{W}$, $\mathbf{w}_m = [w_{1m}, ..., w_{Nm}]^T$, is the precoding vector for UE m in the set $\mathcal{M}$. The received signal of UE m can be rewritten as

$$y_m = \mathbf{h}_m \mathbf{w}_m b_m + \sum_{i \in \mathcal{M}, i \neq m} \mathbf{h}_m \mathbf{w}_i b_i + n_m \,. \tag{3}$$

Let $p_m = b_m b_m^H$ denote the symbol power allocated to UE m across the N TNs. The signal to interference plus noise ratio (SINR) of UE m is then given by

$$\rho_m = \frac{\|\mathbf{h}_m \mathbf{w}_m\|^2 p_m}{\sum_{i \in \mathcal{M}, i \neq m} \|\mathbf{h}_m \mathbf{w}_i\|^2 p_i + \sigma^2}. \tag{4}$$

Thus, the sum rate of the cluster can be expressed as

$$C = \sum_{m \in \mathcal{M}} \log_2(1 + \rho_m). \tag{5}$$

Using zero-forcing precoding, the precoding matrix, $\mathbf{W}$, is obtained as the pseudo-inverse of the channel matrix, $\hat{\mathbf{H}}$, available at the CU.

In order to reduce the complexity, a sub-optimal equal power allocation is considered [11]. As a first step, $\mathbf{W}$ is normalized column-wise, then for any given UE set, $\mathcal{M}$, the power allocation vector is derived as

$$\mathbf{p} = \left\{ \min_{n=1,...N} \frac{P_{\max}}{\sum_{m \in \mathcal{M}} \|w_{nm}\|^2} \right\} \mathbf{1}_{[|\mathcal{M}| \times 1]} \,. \tag{6}$$

By solving the joint power allocation of (6) for every possible UE set $\mathcal{M}$, the chosen UE set $\mathcal{M}^{\text{JT}}$ and $\mathbf{p}^{\text{JT}}$ will be the ones that achieve the highest $\sum_{m=1}^{M} \log_2(1 + \hat{\rho_m})$, where $\hat{\rho_m}$ is derived from (4) by using the obtained $\hat{\mathbf{h}}_m$ at the CU instead of the true channel vector $\mathbf{h}_m$. In the following, this zero-forcing coherent joint transmission scheme is denoted as JT.

B. Coordinated Scheduling

In the considered coordinated scheduling scheme, data to a single UE is only transmitted from its serving TN, which is selected based on the long term channel quality measurements, including pathloss and shadow fading. Hence, user data exchange between TNs is not needed. It is assumed that a TN can transmit data to at most one UE in any given resource slot.

Let $P_m = b_m^H b_m$ denote the transmit power of TN m to UE m, with $P_m \leq P_{\max}$. Then, the SINR for UE m is given as

$$\rho_m = \frac{\left\| h_{mm} \right\|^2 P_m}{\sum_{j=1, j \neq m}^{j=N} \left\| h_{mj} \right\|^2 P_j + \sigma^2}. \tag{7}$$

Thus, the sum rate can be calculated by (5).

UE scheduling and power allocation decisions are jointly made at the CU to control ICI. With the gathered channel matrix, $\hat{\mathbf{H}}$, the CU designs the UE selection indicator matrix $\mathbf{S}$ and the power allocation vector $\mathbf{P} = [P_1, ..., P_n]$, in order to maximize the sum rate subject to per-TN power constraints. Based on [22] and [23], a suboptimal but efficient binary power control (BPC) is considered for this coordinated scheduling scheme, i.e., $P_n = 0$ or $P_{\max}$ for $\forall n \in \{1, ..., N\}$. Then, the relaxed problem becomes an exhaustive binary search. The CU searches all feasible boundary point sets, i.e., $P_n = 0$ or $P_{\max}$ for $\forall n \in \{1, ..., N\}$. The chosen transmit power vector $\mathbf{P}^{\text{CS}}$ will be the one that achieves the highest $\sum_{m=1}^{M} \log_2(1 + \hat{\rho_m})$, where $\hat{\rho_m}$ is derived from (7) by using the obtained $\hat{\mathbf{h}}_m$. In this paper, this scheme is named as CS.

III. Control Channel Models

In this section, we introduce the control channel models considered for single cell transmission and for the cooperative systems under different network architectures, i.e., the centralized, semi-distributed and fully distributed CoMP architectures. We assume that each TN n is linked to one user, i.e., UE n, yet each TN n is potentially serving other UEs in the cluster.

A. *Single Cell Transmission*

Single cell transmission without TN coordination (Fig. 1), denoted as SC, is used as a baseline. For SC transmission, the data blocks sent from the core network to TN n will only contain the data symbol for UE n. All TNs will always be transmitting, if user data is available, even if the channel conditions are poor over the access link. There is no cooperation between TNs, therefore CSI needs not to be shared.

B. *Centralized CoMP Architecture*

The centralized architecture, introduced in [20], [24], is depicted in Fig. 2. Under this architecture, each UE n feeds back its CSI to its serving TN n via access link in the first step. Next, the TNs forward their received local CSI to the CU via backhaul links. Based on the gathered $\hat{\mathbf{H}}$, the CU constructs the precoding matrix for the JT scheme or makes scheduling decisions for the CS scheme. Once the decisions are made, the CU forwards them via backhaul links to each coordinated TN. Hence, backhaul links are used twice, i.e., gathering full CSI and distributing transmission decisions. We assume that the user data distributed from the core network to the CU is fully reliable.

All control channels are modeled to be prone to errors, leading to losing partial CSI of the system at the CU and/or losing precoded user data at the cooperating TNs. The full CSI available at the CU is affected by the LFPs of the access links between each UE n and its serving TN n, as well as the LFPs of the backhaul links between each TN n and the CU. LFPs are modeled as independent binary discrete random variables. Hence the available system channel matrix at CU, $\hat{\mathbf{H}}$, is obtained as

$$\hat{\mathbf{H}} = \mathbf{H} \odot \mathbf{H}^{\text{Access mask}} \odot \mathbf{H}^{\text{Backhaul mask}}, \tag{8}$$

where $\mathbf{H}$ is the perfect system channel matrix. Here, $\mathbf{H}^{\text{Access mask}}$ is a binary mask matrix, where the n^{th} row vector, $\mathbf{H}^{\text{Access mask}}(n,:)$, is either $\mathbf{0}_{[1\times N]}$ with probability $P^{\text{O}}_{n,n}$ or $\mathbf{1}_{[1\times N]}$. $P^{\text{O}}_{n,n}$ is the LFP of the access link over which user n feeds back the CSI to TN n. Also, $\mathbf{H}^{\text{Backhaul mask}}$ is a binary mask matrix, where each row vector, $\mathbf{H}^{\text{Backhaul mask}}(n,:)$, is either $\mathbf{0}_{[1\times N]}$ with probability $P^{\text{C}}_{\text{F}_n}$ or $\mathbf{1}_{[1\times N]}$. Here, $P^{\text{C}}_{\text{F}_n}$ is the LFP of the backhaul link where the CSI is forwarded from TN n to the CU.

For the JT scheme, the user data distributed from the CU to TN n, x_n, contains the precoded data symbols for the scheduled UEs, i.e., $x_n = \mathbf{W}(n,:) \times \mathbf{b} = \sum_{m\in\mathcal{M}} w_{nm} b_m$. Let $P^{\text{D}}_{\text{F}_n}$ denote the LFP of the backhaul links where the precoded data symbols are distributed from the CU to TN n. Similarly, to model the data loss via backhaul links to each TN, a binary mask matrix, $\mathbf{W}^{\text{Backhaul mask}}$, is applied to the precoding matrix designed at the CU, $\mathbf{W}$, as

$$\hat{\mathbf{W}} = \mathbf{W} \odot \mathbf{W}^{\text{Backhaul mask}}, \tag{9}$$

which erases each row vector of $\mathbf{W}$ independently, with a probability of $P^{\text{D}}_{\text{F}_n}$. The SINR of the scheduled UEs can be derived by substituting $\hat{\mathbf{W}}$ into (4), the sum rate can then be obtained from (5).

Example 1. A cooperative cluster comprises of $N = 3$ TNs, as shown in Fig. 2. All UEs feed back the channel state vector to their serving TN. Then, each TN n forwards the received local channel state vector via backhaul links to the CU. Assume that there are link failures on the access link between UE 2 and TN 2, and the backhaul link from TN 3 to the CU. Then, according to (8), the full CSI available at the CU, $\hat{\mathbf{H}}$, can be modeled as

$$\hat{\mathbf{H}} = \begin{bmatrix} \mathbf{h}_1 \\ \mathbf{h}_2 \\ \mathbf{h}_3 \end{bmatrix} \odot \begin{bmatrix} 1 & 1 & 1 \\ 0 & 0 & 0 \\ 1 & 1 & 1 \end{bmatrix} \odot \begin{bmatrix} 1 & 1 & 1 \\ 1 & 1 & 1 \\ 0 & 0 & 0 \end{bmatrix}.$$

Based on $\hat{\mathbf{H}}$ the precoding matrix $\mathbf{W}$ is designed at the CU. Considering a link failure on the backhaul link between the CU and TN 1 when the precoded user data is distributed from the CU to all TNs,$\hat{\mathbf{W}}$ becomes

$$\hat{\mathbf{W}} = \mathbf{W} \odot \begin{bmatrix} 0 & 0 & 0 \\ 1 & 1 & 1 \\ 1 & 1 & 1 \end{bmatrix}.$$

For the CS scheme, where data to a single UE is only transmitted from its serving TN, the data loss due to backhaul unreliability is modeled as

$$\hat{b}_n = b_n b_n^{\text{mask}}. \tag{10}$$

Here, b_n^{mask} is a binary mask variable which erases the data symbol of UE n with probability $P_{\text{F}_n}^{\text{D}}$. Thus, the SINR of each UE n can be calculated by substituting $\mathbf{P}^{\text{mask}}$ into (7), where the n^{th} element, P_n^{mask}, is derived by $P_n^{\text{mask}} = b_n^{\text{mask}} P_n^{\text{CS}}$.

C. Semi-distributed CoMP Architecture

The semi-distributed architecture, introduced in [25], [26], is depicted in Fig. 3. Under this architecture, each user feeds back the CSI vector to its serving TN. Then, the received local CSI vectors are shared between TNs via interconnecting backhaul links. Therefore, each TN n receives $N-1$ non-local CSI vectors from $N-1$ coordinated TNs via backhaul links, thus acquiring $\hat{\mathbf{H}}_n$, which can be modeled by

$$\hat{\mathbf{H}}_n = \mathbf{H} \odot \mathbf{H}^{\text{Access mask}} \odot \mathbf{H}_n^{\text{Backhaul mask}}, \tag{11}$$

where $\mathbf{H}^{\text{Access mask}}$ is a binary mask matrix defined in (8), modeling the link failure of the access links. Here, $\mathbf{H}_n^{\text{Backhaul mask}}$ is a binary mask matrix for TN n modeling the effect of backhaul link failures. Similarly to (8), the m^{th} row vector, $\mathbf{H}_n^{\text{Backhaul mask}}(m,:)$, is either $\mathbf{0}_{[1\times N]}$ with probability $P_{\text{F}_{m,n}}$ or $\mathbf{1}_{[1\times N]}$, with $m \neq n$. Note that the local CSI vector for each TN n, is directly fed back from its own

UE n. Hence, the n^{th} row of $\hat{\mathbf{H}}_n$ will not be affected by the LFP of backhaul links. Thus, the n^{th} row of $\mathbf{H}_n^{\text{Backhaul mask}} = \mathbf{1}_{[1\times N]}$ with probability 1.

Assume that user data is safely received at each TN from the core network. Based on the gathered $\hat{\mathbf{H}}_n$, each cooperating TN n acts as a CU, independently designing its own precoding weights and the power allocation vector for JT, or making scheduling decisions for CS. Transmission decisions are then locally applied to the user data at each TN.

For the JT scheme, the data blocks, sent from the core network to TN n, contain all data symbols for the scheduled UEs in the cluster, $d_n = [b_1, ..., b_m]$. Each TN n independently designs the precoding matrix $\mathbf{W}_n$ based on the gathered system matrix $\hat{\mathbf{H}}_n$. The n^{th} row of $\mathbf{W}_n$, i.e., $\mathbf{W}_n(n,:)$, is then chosen by TN n as the precoding vector for mapping the user data symbols into the transmit signal. Therefore, the system precoding matrix will be

$$\hat{\mathbf{W}} = \begin{bmatrix} \mathbf{W}_1(1,:) \\ \mathbf{W}_2(2,:) \\ \vdots \\ \mathbf{W}_N(N,:) \end{bmatrix}. \tag{12}$$

The SINR of the scheduled UEs can be derived by substituting $\hat{\mathbf{W}}$ into (4). Finally, the sum rate can then be obtained from (5).

Example 2. A cooperative cluster comprises of $N = 3$ TNs, as shown in Fig. 3. Consider modeling the gathered $\hat{\mathbf{H}}_1$ at TN 1. Firstly, all UEs feed back the local channel state vector to their serving TN. Hence, TN 1 receives the channel state vector $\mathbf{h}_1$ from UE 1, through the access link. Then, TN 2 and TN 3 share $\mathbf{h}_2$ and $\mathbf{h}_3$ with TN 1 through unreliable backhaul links. Assume that there are link failures on the access link between UE 2 and TN 2, and on the backhaul link between TN 3 to TN 1. Then, according to (11), $\hat{\mathbf{H}}_1$ can be modeled as

$$\hat{\mathbf{H}}_1 = \begin{bmatrix} \mathbf{h}_1 \\ \mathbf{h}_2 \\ \mathbf{h}_3 \end{bmatrix} \odot \begin{bmatrix} 1 & 1 & 1 \\ 0 & 0 & 0 \\ 1 & 1 & 1 \end{bmatrix} \odot \begin{bmatrix} 1 & 1 & 1 \\ 1 & 1 & 1 \\ 0 & 0 & 0 \end{bmatrix}.$$

Based on $\hat{\mathbf{H}}_1$, TN 1 designs the precoding matrix $\mathbf{W}_1$. Then, the first row of $\mathbf{W}_1$, i.e., $\mathbf{W}_1(1,:)$

will be chosen as the precoding vector for TN 1. The system precoding matrix $\hat{\mathbf{W}}$ is then derived from (12).

For the CS scheme, the downlink data block, d_n, which is distributed from the core network to each TN n, contains only the data symbol of its own UE. Thus, $d_n = b_n$. Based on available $\hat{\mathbf{H}}_n$, each TN n designs the transmit power vector $\mathbf{P}_n^{\text{CS}}$. The n^{th} element of $\mathbf{P}_n^{\text{CS}}$, i.e., $\mathbf{P}_n^{\text{CS}}(n)$ is then chosen by TN n as the transmit power for UE n. Thus, the system transmit power vector will be

$$\hat{\mathbf{P}}^{\text{CS}} = \left[\mathbf{P}_n^{\text{CS}}(1),\, \mathbf{P}_n^{\text{CS}}(2),\, \ldots,\, \mathbf{P}_N^{\text{CS}}(N)\right]. \tag{13}$$

The SINR of the scheduled UEs can be derived by substituting $\hat{\mathbf{P}}^{\text{CS}}$ into (7).

D. Fully Distributed CoMP Architecture

The fully distributed architecture, introduced in [21], [27], is depicted in Fig. 4. This architecture differs from the semi-distributed architecture (Section III-C) in the way TN n acquires the full CSI matrix $\hat{\mathbf{H}}_n$. All UEs in the cluster broadcast their local CSI vectors to all TNs, therefore, any row of the local gathered system channel matrix, $\mathbf{h}_m$, can be lost due to the LFP of the access links between UE m and TN n. Hence, $\hat{\mathbf{H}}_n$ can be modeled by

$$\hat{\mathbf{H}}_n = \mathbf{H} \odot \mathbf{H}_n^{\text{Access mask}}, \tag{14}$$

where $\mathbf{H}_n^{\text{Access mask}}$ is a binary mask matrix for TN n modeling the link failures of the access links between TN n and all UEs. Here, $P_{n,m}^{\text{O}}$ is the outage probability between UE m and TN n. Similarly to (8), the m^{th} row vector, $\mathbf{H}_n^{\text{Access mask}}(m,:)$, is either $\mathbf{0}_{[1\times N]}$ with probability $P_{n,m}^{\text{O}}$ or $\mathbf{1}_{[1\times N]}$, with $n \neq m$.

IV. Control Channel Reliability Analysis

In this section we analyze the probability of a certain TN n staying silent in a resource slot, P_n^{S}, due to unreliable control channels. This may cause some UEs unserved, or, as a worst-case scenario, impede all transmission with probability

$$P^{\text{W}} = \prod_{n=1}^{N} P_n^{\text{S}}. \tag{15}$$

The LFP of the control channels can be evaluated in terms of outage probability of the wireless channels. It is assumed that the UEs use orthogonal control channels for CSI feedback, therefore, outage probability is the probability that the instantaneous signal-to-noise ratio (SNR), x, is below that required for adequate reception [28]. The short-term variability of mobile radio signals can usually be described statistically with enough accuracy to be useful in mobile radio system analysis. If the desired SNR has a probability density function, $p_\gamma(z)$, then the probability that adequate reception will not be achieved, P_{out}, is

$$P_{\text{out}}(x) = \Pr(\gamma < x) = \int_0^x p_\gamma(z)dz\,, \tag{16}$$

where $\Pr(.)$ denotes probability.

In this section, we also provide closed form equations for P_n^{S} for different transmission schemes under different architectures, when the control channels are modeled with Rayleigh fading. Under Rayleigh fading, the received signal power is exponentially distributed, and the variations of the instantaneous SNR also follow an exponential distribution. Therefore, the outage probability can be obtained from

$$P_{\text{out}}\left(x\right) = 1 - \exp\left(-\frac{x}{\Omega\left(d\right)}\right), \tag{17}$$

where x is the minimum required SNR for adequate reception, and $\Omega\left(d\right)$ is the mean SNR level at distance d from the transmitter. Although more sophisticated channel models provide better statistical description, we use Rayleigh fading to maintain simplicity and tractability.

A. Single Cell Transmission

As discussed in III-A, a certain TN n will always be transmitting, regardless of the reliability of the control channels. Therefore, P_n^{S} can be expressed as

$$P_n^{\text{S}} = 0. \tag{18}$$

B. Centralized CoMP architecture

Coherent Joint Transmission: Considering the JT scheme under the centralized architecture, based on the control channel model described in Section III-B, TN n will stay silent if

Case 1. All CSI vectors are lost at the CU so that no transmission decisions will be distributed from the CU to all TNs, otherwise,

Case 2. The precoded user data distributed from the CU to TN n is lost.

The probability that Case 1 happens is $\prod_{n=1}^{N}\left[P_{\mathrm{F}_n}^{\mathrm{C}}+\left(1-P_{\mathrm{F}_n}^{\mathrm{C}}\right)\cdot P_{n,n}^{\mathrm{O}}\right]$, where $P_{\mathrm{F}_n}^{\mathrm{C}}$ is the LFP of the backhaul link between TN n and the CU when TN n forwards the local CSI to the CU, and $P_{n,n}^{\mathrm{O}}$ is the LFP of the access link between UE n and TN n, when UE n feeds back the CSI to TN n. Case 2 happens with probability $P_{\mathrm{F}_n}^{\mathrm{D}}$, where $P_{\mathrm{F}_n}^{\mathrm{D}}$ is the LFP between the CU and TN n, when the CU distributes precoded user data to TN n (see Fig. 5 for corresponding illustration). Therefore, the probability of TN n staying silent, P_n^{S}, for the JT scheme under the centralized architecture can be expressed as

$$P_n^{\mathrm{S}}=P_{\mathrm{F}_n}^{\mathrm{D}}+(1-P_{\mathrm{F}_n}^{\mathrm{D}})\prod_{n=1}^{N}\left[P_{\mathrm{F}_n}^{\mathrm{C}}+\left(1-P_{\mathrm{F}_n}^{\mathrm{C}}\right)\cdot P_{n,n}^{\mathrm{O}}\right]. \tag{19}$$

Consider a special case, where the control channels, i.e., the access and backhaul links, are modeled as orthogonal Rayleigh fading channels. Then, based on (17), P_n^{S} in (19) can be written as:

$$P_n^{\mathrm{S}}=\left[1-\exp\left(\lambda^{\mathrm{D}}\left(d_{\mathrm{CU},n}\right)\right)\right]+\exp\left(\lambda^{\mathrm{D}}\left(d_{\mathrm{CU},n}\right)\right)\prod_{n=1}^{N}\left[1-\exp\left(\lambda^{\mathrm{C}}\left(d_{\mathrm{CU},n}\right)+\lambda^{\mathrm{O}}\left(d_{n,n}\right)\right)\right], \tag{20}$$

where each link can be characterized with $\lambda\left(d\right)=-\frac{x}{\Omega\left(d\right)}$. Here, $d_{\mathrm{CU},n}$ is the distance between TN n and the CU, and $d_{n,n}$ is the distance between UE n and TN n.

Coordinated Scheduling: In case of the CS scheme, it is possible that the TN will not transmit in the current resource block even if CSI sharing is not affected by the failure of control channels. This is because BPC is performed to control the interference, depending on the current channel conditions. Hence, TN n will stay silent if

Case 1. The TN will not transmit in the current resource block, due to BPC, otherwise,

Case 2. The user data distributed from the CU to TN n is lost.

The probability that Case 1 happens is indicated as P_n^{NS}, while Case 2 happens with probability $P_{\mathrm{F}_n}^{\mathrm{D}}$. Therefore, P_n^{S} for the CS scheme under centralized architecture can be expressed as

$$P_n^{\mathrm{S}}=P_{\mathrm{F}_n}^{\mathrm{D}}+(1-P_{\mathrm{F}_n}^{\mathrm{D}})P_n^{\mathrm{NS}}. \tag{21}$$

Consider a special case, where the control channels, i.e., the access and backhaul links, are modeled as Rayleigh fading channels, then, based on (17), P_n^{S} in (21) can be written as:

$$P_n^{\mathrm{S}}=\left[1-\exp\left(\lambda^{\mathrm{D}}\left(d_{\mathrm{CU},n}\right)\right)\right]+\exp\left(\lambda^{\mathrm{D}}\left(d_{\mathrm{CU},n}\right)\right)P_n^{\mathrm{NS}}. \tag{22}$$

C. Semi-distributed CoMP architecture

Coherent Joint Transmission: In case of the JT scheme, TN n will stay silent if all CSI vectors are lost at TN n. The probability that the local CSI vector ($\mathbf{h}_n$) fed back by its own user, UE n, gets lost is $P^{\text{O}}_{n,n}$, which is the LFP of the access link between UE n and TN n. A non-local CSI ($\mathbf{h}_m$ with $m \neq n$) can be lost at TN n if $\mathbf{h}_m$ is not received at TN m via access links from UE m, or $\mathbf{h}_m$ does not reach TN n via backhaul links from TN m (see Fig. 6 for corresponding illustration). Hence, the probability that all non-local CSI vectors are lost at TN n is $\prod_{i=1,i\neq n}^{N}\left[P^{\text{O}}_{i,i} + \left(1 - P^{\text{O}}_{i,i}\right)\cdot P_{\text{F}_{n,i}}\right]$. Therefore, P^{S}_n for the JT scheme under semi-distributed architecture can be expressed as

$$P^{\text{S}}_n = P^{\text{O}}_{n,n}\prod_{i=1,i\neq n}^{N}\left(P^{\text{O}}_{i,i} + \left(1 - P^{\text{O}}_{i,i}\right)\cdot P_{\text{F}_{n,i}}\right). \tag{23}$$

Consider a special case, where the control channels, i.e., the access and backhaul links, are modeled as Rayleigh fading channels without interference, then, based on (17), P^{S}_n in (23) can be written as:

$$P^{\text{S}}_n = \left(1 - \exp\left(\lambda^{\text{O}}\left(d_{n,n}\right)\right)\right)\prod_{i=1,i\neq n}^{N}\left(1 - \exp\left(\lambda^{\text{O}}\left(d_{n,n}\right) + \lambda_{\text{F}}\left(d_{n,i}\right)\right)\right). \tag{24}$$

Coordinated Scheduling: Considering the CS scheme under the semi-distributed architecture, P^{NS}_n will depend on the LFP of the backhaul links interconnecting the TNs and on the LFP of the access links. Thus P^{S}_n can be obtained as

$$P^{\text{S}}_n = P^{\text{NS}}_n. \tag{25}$$

D. Fully distributed CoMP architecture

Coherent Joint Transmission: In case of the JT scheme P^{S}_n depends on whether CSI has reached TN n. Hence, TN n will stay silent if all CSI vectors, sent from the UEs, are lost at TN n. All UEs broadcast their CSI and the LFP of the access links between UE m and TN n is given by $P^{\text{O}}_{n,m}$ (see Fig. 7 for corresponding illustration). Therefore, P^{S}_n for the JT scheme under fully distributed architecture can be expressed as

$$P^{\text{S}}_n = \prod_{m=1}^{M} P^{\text{O}}_{n,m}. \tag{26}$$

Consider a special case, where the control channels, i.e., the access and backhaul links, are modeled as Rayleigh fading channels, then, based on (17), P^{S}_n in (26) can be written as:

$$P_n^{\mathrm{S}} = \prod_{m=1}^{M} \left(1 - \exp\left(\lambda^{\mathrm{O}}\left(d_{n,m}\right)\right)\right). \quad (27)$$

Coordinated Scheduling: Considering the CS scheme under the fully distributed architecture, P_n^{S} can be calculated using (25). In this case, however, P_n^{NS} will depend on the LFPs of the access links between the UEs and TN n.

V. PERFORMANCE EVALUATION

We consider the downlink of a CoMP cluster with $N = 2$ and $N = 3$ neighboring sectors respectively. For each cluster size, N, $M = N$ single-antenna UEs are grouped together using a particular resource slot. The cluster radius R is 500 m. The path loss model is $PL(d) = 128.1 + 37.6 \log_{10}(d)$ in dB, with d given in km. The system SNR is set to 18 dB, which is defined as the received SNR at the boundary of the cell, assuming full power transmission $P_{\max}$ from the TN, accounting only for pathloss $PL(R)$ and ignoring fast fading [20]. The noise power, σ^2, is set to -135 dBm.

To simplify our investigations, we assume that the UEs are collectively moving from their cell centers to the cluster center along the dashed line as depicted in Fig. 8. SC transmission without TN coordination, denoted as Single Cell, is used as baseline. For each of the analyzed CoMP architectures, i.e., the centralized, semi-distributed and fully distributed versions, the considered JT, CS, and SC transmission schemes are evaluated and compared. For each position, the average sum rate, $\overline{C}$, is obtained by averaging the sum rate of the cluster, obtained from (5), over $1 \cdot 10^5$ independent UE set realizations. The normalized distance of the UEs from the cell center is $\frac{d}{R}$.

A. Average Sum Rate with Perfect Control Information

Fig. $10a$ and Fig. $10b$ plot the average sum rate of the cluster, $\overline{C}$, for different transmission schemes versus the normalized distance, with cluster size $N = 2$ and $N = 3$ respectively. In this case all access and backhaul links are modeled to be completely reliable, to illustrate how much performance gain is offered by the investigated CoMP schemes. Under such conditions the architecture has no effect on the performance. The performance gain offered by the cooperative schemes is growing as interference becomes more severe when UEs are near the cluster center.

B. Performance with Unreliable Control Information

Access Link Failure Probability: For both access and backhaul links, shadowing is ignored during the simulations. Only path loss and Rayleigh fading is considered, therefore, the signal power envelope is exponentially distributed at a given distance d. We assume that the UEs use orthogonal control channels during CSI feedback with a fixed transmit power. Consider the CSI feedback from UE m to TN n with distance d , the LFP of this access link can be evaluated by (17), where the mean SNR can be obtained by [29]

$$\Omega\left(d\right) = \frac{P_{\mathrm{t}}}{PL(d)\sigma^2}. \tag{28}$$

We assume that the minimum required SNR for adequate reception, $x = \frac{P_{\mathrm{t}}}{PL(d_{\max})\sigma^2}$. Since the control channels for CSI-feedback are considered to be interference-free, the LFP of the access link between each UE m and each TN n, $P^{\mathrm{O}}_{n,m}$, in equations (19) and (23) is independent of the cluster size, N. In Fig. 9, the LFP of the access link between a certain UE and its serving TN, $P^{\mathrm{O}}_{n,n}$, is plotted versus the normalized distance $\frac{d}{R}$.

The Probability of a TN Staying Silent: For a symmetric CoMP cluster shown in Fig. 8, all backhaul links are assumed to have the same LFP, P_{F}. Since the UEs are moving collectively, all access links between the UEs and their serving TNs are characterized with the same outage probability, P^{O}, and all access channels between the UEs and their neighboring TNs are characterized with the same outage probability, $P^{\mathrm{O}}_{n,m}$. Note that P^{O} and $P^{\mathrm{O}}_{n,m}$ are functions of distance d, being the same value for all UEs in each realization. In this case, the equations (19), (21), (23) and (26) are reduced to the following forms. For JT under the centralized architecture:

$$P^{\mathrm{S}}_{n} = P_{\mathrm{F}} + (1-P_{\mathrm{F}})\left[P_{\mathrm{F}} + (1-P_{\mathrm{F}})\,P^{\mathrm{O}}\right]^{N}\ . \tag{29}$$

For CS under the centralized architecture:

$$P^{\mathrm{S}}_{n} = P_{\mathrm{F}} + (1-P_{\mathrm{F}})P^{\mathrm{NS}}_{n}\ . \tag{30}$$

For JT under the semi-distributed architecture:

$$P^{\mathrm{S}}_{n} = P^{\mathrm{O}}\left(P^{\mathrm{O}} + \left(1-P^{\mathrm{O}}\right)P_{\mathrm{F}}\right)^{N-1}\ . \tag{31}$$

For JT under the fully distributed architecture:

$$P^{\mathrm{S}}_{n} = \prod_{m=1}^{M} P^{\mathrm{O}}_{n,m}\,. \tag{32}$$

If we consider the special case of modeling the wireless links with Rayleigh fading, (29) - (32) will have the following form:

$$P_n^{\mathrm{S}} = \left[1 - \exp\left(\lambda_{\mathrm{F}}\left(d_{\mathrm{CU},n}\right)\right)\right] + \exp\left(\lambda_{\mathrm{F}}\left(d_{\mathrm{CU},n}\right)\right)\left[1 - \exp\left(\lambda_{\mathrm{F}}\left(d_{\mathrm{CU},n}\right) + \lambda^{\mathrm{O}}\left(d_{n,n}\right)\right)\right]^{N}, \tag{33}$$

$$P_n^{\mathrm{S}} = \left[1 - \exp\left(\lambda_{\mathrm{F}}\left(d_{\mathrm{CU},n}\right)\right)\right] + \exp\left(\lambda_{\mathrm{F}}\left(d_{\mathrm{CU},n}\right)\right) P_n^{\mathrm{NS}}, \tag{34}$$

$$P_n^{\mathrm{S}} = \left(1 - \exp\left(\lambda^{\mathrm{O}}\left(d_{n,n}\right)\right)\right)\left[\left(1 - \exp\left(\lambda^{\mathrm{O}}\left(d_{n,n}\right)\right)\right) + \exp\left(\lambda^{\mathrm{O}}\left(d_{n,n}\right)\right)\left(1 - \exp\left(\lambda_{\mathrm{F}}\left(d_{\mathrm{CU},n}\right)\right)\right)\right]^{N-1}, \tag{35}$$

$$P_n^{\mathrm{S}} = \prod_{m=1}^{M} \left(1 - \exp\left(\lambda^{\mathrm{O}}\left(d_{n,m}\right)\right)\right). \tag{36}$$

Note, that P^{S} does not directly limit $\overline{C}$, since the silence of a TN also decreases the inter-cell interference in the neighboring cells. Fig. 11 and Fig. 12 show the probability of a certain TN n staying silent in a resource slot, P_n^{S}, versus the normalized distance, for each transmission scheme and system architecture. The backhaul LFP P_{F} is set to 0.1.

We can see that in the region where the UEs are close to their serving TNs, a certain TN will stay silent with a significantly higher probability under the centralized architecture with both JT and CS schemes. From (29)-(32) it can be seen that P_n^S for the JT scheme under centralized architecture is dominated by backhaul LFP, P_F, while the impact of backhaul LFP on P_n^S is much less under the semi-distributed architecture. Backhaul LFP has no impact on the performance under the fully-distributed architecture.

For the JT scheme under the semi-centralized architecture, P^{S} shows a similar trend as with SC transmission. However, under the fully distributed architecture P^{S} drops after an initial rise as the UEs get closer to the cluster center. This is due to the fact that the UEs use orthogonal access links and the broadcasted CSI vectors reach the neighboring TNs with a higher probability, since the LFP of the access links is a function of their access distance. For the JT scheme, P^{S} appears to be inversely proportional to the cluster size under all architectures.

For the CS scheme, P^{S} reaches the highest values under the fully distributed architecture as the UEs get closer to the cluster center. This is due to the fact that the BPC algorithm reduces interference by keeping more TNs silent on average. For the CS scheme, P^{S} appears to be directly proportional to the cluster size under all architectures.

Average Sum Rate Evaluation: Fig. 13 and Fig. 14 plot the average sum rate of the cluster, $\overline{C}$, for different transmission schemes versus the normalized distance with cluster size $N = 2$ and $N = 3$ respectively. It is assumed that all backhaul links have the same LFP, $P_{\mathrm{F}} = 0.1$. As shown in Fig. 9, under the assumption of fixed transmit power at each UE, the LFP of the access links between the UEs and the TNs is a function of distance d. Compared to the case where all control channels are assumed to be fully reliable (Fig. 10), the performance of all CoMP schemes declines. It is apparent, however, that the control channel architecture of the cluster has a significant effect on the average sum rate. Under the centralized architecture the performance of the CoMP schemes is worse than SC transmission, since the backhaul link between the TNs and the CU is prone to errors, even when the UEs are close to their serving TN. As the UEs move towards the cluster center, the path loss over the access link and the interference get larger, thus the performance of SC transmission drops sharply. Initially, the JT scheme under semi-distributed architecture offers the highest achievable sum rate, however, this gain diminishes quickly as control channel unreliability over the access link grows. As the UEs get closer to the cluster center, the distance between the UEs and the neighboring TNs gets smaller. In this region the JT scheme offers the best performance under the fully distributed architecture, because CSI is shared over the access links. However, the CS scheme doesn't perform well near the cluster center under the fully distributed architecture, because each TN decides not to transmit with high probability.

Fig. 15 and Fig. 16 plot $\overline{C}$ against varying backhaul LFP, P_{F}, when the normalized distance of the UEs from the cell centers is 0.4. The performance of the SC transmission and the fully distributed architecture does not depend on P_{F}, since the control signals are only transmitted through the access links. The centralized architecture is the most sensitive to backhaul LFP, and if the backhaul links fail with certainty, no transmission is possible. The performance of the semi-distributed architecture converges to SC transmission, because if the gathered system channel matrix at TN n only contains information from UE n with high probability, the application of precoding and scheduling algorithms becomes redundant.

VI. CONCLUSIONS

In this paper, the effects of control channel reliability on the performance of a cluster of cooperative transmission nodes has been studied. In particular, two transmission schemes, coherent joint transmission and coordinated scheduling, were evaluated under the centralized, semi-distributed and fully distributed CoMP architectures. The scenarios were assessed in terms of average sum rate of the cluster, and traditional single cell transmission served as a baseline for comparison. Analytical results were derived to show how unreliable backhaul links and unreliable access links affect quality of service. Numerical results show that cooperative transmission techniques have the potential to improve the performance of the cellular system, in terms of sum rate. However, the performance of the system highly depends on the reliability of the control channels, and more importantly, on the probability of successful channel state information exchange. Although all examined scenarios suffer from performance degradation as intra-cell interference increases, the coherent joint transmission scheme proved to be more robust under the fully distributed architecture. With the coherent joint transmission scheme also higher sum rates can be achieved. The semi-distributed and fully distributed architectures are less sensitive to backhaul unreliability, however, they require all cooperating TNs to be capable of performing precoding or making scheduling decisions.

Acknowledgment

This work is supported by the Swedish Agency for Innovation Systems (VINNOVA), within the P36604-1 MAGIC project and the Swedish Research Council VR under the project 621-2009-4555 Dynamic Multipoint Wireless Transmission. Part of this work has been performed in the framework of the FP7 project ICT-317669 METIS, which is partly funded by the European Union. The authors would like to acknowledge the contributions of their colleagues in METIS, although the views expressed are those of the authors and do not necessarily represent the project.

References

[1] D. McQueen, "The momentum behind LTE adoption," *IEEE Commun. Mag.*, vol. 47, no. 2, pp. 44–45, Feb. 2009.

[2] C. Gandarillas, V. Iglesias, M. Aparicio, E. Mino-Díaz, P. Olmos, "A new approach for improving indoor LTE coverage," in *Proc. IEEE GLOBECOM Workshops 2011*, pp. 1330 – 1335, Dec. 2011.

[3] V. Chandrasekhar, J. G. Andrews and A. Gatherer, "Femtocells Networks: A Survey," *IEEE Commun. Mag.*, vol. 46, no. 9, pp. 59–67, Jun. 2008.

[4] A. Ghosh, J. G. Andrews, N. Mangalvedhe, R. Ratasuk, B. Mondal, M. Cudak, E. Visotsky, T. A. Thomas, P. Xia, H. S. Jo, H. S. Dhillon, T. D. Novlan, "Heterogeneous Cellular Networks: From Theory to Practice," *IEEE Commun. Mag.,* vol. 50, no. 6, pp. 54–64, Jun. 2012.

[5] G. Boudreau, J. Panicker, N. Guo, R. Chang, N. Wang, and S. Vrzic, "Interference Coordination and Cancellation for 4G Networks," *IEEE Commun. Mag.*, vol. 47, no. 4, pp. 74–81, Apr. 2009.

[6] A. Barbieri, P. Gaal, S. Geirhofer, T. Ji, D. Malladi, Y. Wei, F. Xue, "Coordinated downlink multi-point communications in heterogeneous cellular networks," in *Proc. IEEE ITA 2012*, San Diego, CA, Feb. 2012.

[7] M. Sawahashi, Y. Kishiyama, A. Morimoto, D. Nishikawa, and M. Tanno, “Coordinated multipoint transmission/reception techniques for LTE-advanced [Coordinated and Distributed MIMO],” *IEEE Wireless Communications*, vol. 17, no. 3, pp. 26-34, Jun. 2010.

[8] D. Gesbert, S. Hanly, H. Huang, et al., “Multi-cell MIMO cooperative networks: a new look at interference,” *IEEE J. Select. Areas Commun.*, vol. 28, pp. 1380-1408, Dec. 2010.

[9] D. Lee, H. Seo, B. Clerckx, E. Hardouin, D. Mazzarese, S. Nagata, and K. Sayana, “Coordinated multipoint transmission and reception in LTE-advanced: deployment scenarios and operational challenges,” *IEEE Commun. Mag.*, vol. 50, no. 2, pp. 148-155, Feb. 2012.

[10] S. A. Ramprashad, H. C. Papadopoulos, A. Benjebbour, Y. Kishiyama, N. Jindal, and G. Caire, “Cooperative cellular networks using multi-user MIMO: tradeoffs, overheads, and interference control across architectures,” *IEEE Commun. Mag.*, vol. 49, no. 5, pp. 70-77, May 2011.

[11] A. Papadogiannis, H. J. Bang, D. Gesbert and E. Hardouin, “Efficient selective feedback design for multicell cooperative networks,” *IEEE Trans. Vehicular Techn.*, vol. 60, no. 1, pp. 196–205, Jan. 2011.

[12] P. Marsch and G. Fettweis (editors), *Coordinated Multi-Point in Mobile Communications - From Theory to Practice*, Cambridge University Press, 2011.

[13] D.L. Villa, C.U. Castellanos, I.Z. Kovacs, F. Frederiksen, K.I. Pedersen, “Performance of Downlink UTRAN LTE under Control Channel Constraints,” in *IEEE VTC 2008*, pp. 2512-2516, May 2008.

[14] L. Zhang, Z. He, K. Niu, X. Wang, P. Skov, “Impact of Control Channel Constraints on Downlink Performance Comparison of MIMO Transmission Schemes in 3GPP LTE,” in *Proc. IEEE PIMRC 2009*, pp. 2075 - 2079, Sept. 2009.

[15] B. Maham, A. Behnad, M. Debbah, ”Analysis of Outage Probability and Throughput for Half-Duplex Hybrid-ARQ Relay Channels,” *IEEE Trans. Vehicular Techn.*, vol. 61 , no. 7, pp. 3061 - 3070, Sept. 2012.

[16] A. Papadogiannis, T. Svensson, “Performance Analysis of Centralized Relay Selection with Unreliable Control Information,” in *Proc. IEEE VTC 2012*, Québec City, Canada, Sept. 2012.

[17] O. Tipmongkolsilp, S. Zaghloul, A. Jukan, “The evolution of cellular backhaul technologies: Current issues and future trends,” *IEEE Commun. Surveys Tut.*, vol. 13, no. 1, pp. 97–113, 1st Quart., 2011.

[18] M. Coldrey, H. Koorapaty, J.-E. Berg, Z. Ghebretensaé, J. Hansryd, A. Derneryd, S. Falahati, “Small-Cell Wireless Backhauling,” in *Proc. IEEE VTC 2012*, Québec City, Canada, Sept. 2012.

[19] Z. Mayer, J. Li, A. Papadogiannis, T. Svensson, “On the Impact of Backhaul Channel Reliability on Cooperative Wireless Networks,” in *Proc. IEEE ICC 2013*, Budapest, Hungary, Jun. 2013. To appear.

[20] J. Li, A. Papadogiannis, R. Apelfröjd, T. Svensson, and M. Sternad, “Performance Evaluation of Coordinated Multi-Point Transmission Schemes with Predicted CSI,” in *Proc. IEEE PIMRC 2012*, Sydney, Australia, Sept. 2012.

[21] A. Papadogiannis, E. Hardouin, and D. Gesbert, “Decentralising multicell cooperative processing: A novel robust framework,” *EURASIP J. Wireless Commun. Netw.*, vol. 2009, p. 10, Aug. 2009.

[22] A. Gjendemsjø, D. Gesbert, G. Øien and S. Kiani, “Binary power control for sum rate maximization over multiple interfering links,” *IEEE Trans. Wireless Commun.*, vol. 7, no. 8, pp. 3164–3173, Aug. 2008.

[23] J. Li, T. Svensson, C. Botella, T. Eriksson, X. Xu and X. Chen, “Joint scheduling and power control in coordinated multi-point clusters,” in *Proc. IEEE VTC 2011*, San Francisco, USA, Sept. 2011.

[24] H. Zhang and H. Dai, “Cochannel interference mitigation and cooperative processing in downlink multicell multiuser MIMO networks,” *EURASIP J. Wireless Comm. and Netw.*, vol. 2004, no. 2, pp. 222-235, Dec. 2004.

[25] V. Jungnickel, L. Thiele, T. Wirth, T. Haustein, S. Schiffermüller, A. Forck, S. Wahls, S. Jaeckel, S. Schubert, S. Gäbler, C. Juchems, F. Luhn, R. Zavrtak, H. Droste, G. Kadel, W. Kreher, J. Mueller, W. Stoermer, and G. Wannemacher, "Coordinated multipoint trials in the downlink," in *Proc. IEEE GLOBECOM Workshops*, pp. 1-7, Dec. 2009.

[26] L. Scalia, T. Biermann, C. Choi, K. Kozu, and W. Kellerer, "Power-efficient mobile backhaul design for CoMP support in future wireless access systems," in *Proc. IEEE Computer Commun. Workshops (INFOCOM WKSHPS)*, pp. 253 - 258, April 2011.

[27] R. Fritzsche and G. P Fettweis, "CSI distribution for joint processing in cooperative cellular networks," in *Proc. IEEE VTC Fall*, pp. 1-5, Sept. 2011.

[28] A.J. Goldsmith, *Wireless Communications*, Cambridge University Press, New York, 2005.

[29] K.W. Sowerby, "Outage probability in mobile radio systems," *Ph.D. thesis*, The University of Auckland, Auckland, New Zealand, Feb. 1989.

[30] J. S. Engel, "The effects of cochannel interference on the parameters of a small-cell mobile telephone system", *IEEE Trans. Veh. Tech.*, vol. 18, no. 3, pp. 110-116, Nov. 1969.

List of Figures

Figure 8, The simulated movement of the UEs, with cluster size$=3$, considered in numerical performance evaluation. As the UEs approach the cluster center, the LFP between them and the TNs grows, impeding CSI feedback. Heightened interference also hampers data transmission.

Figure 9, The LFP of the control channel over the access link used for CSI feedback, P_{out}, vs. normalized distance, $\frac{d}{R}$, between UE n and its serving TN n. It is assumed that the control channels are orthogonal for different users.

Figure 10, The average sum rate of the cluster, $\overline{C}$, vs. normalized distance, $\frac{d}{R}$, for *a)* Cluster size $=2$, *b)* Cluster size$=3$. It is assumed that the control channels are completely reliable, i.e., the LFP of all access links, $P^{\text{O}}_{n,m}$, and the LFP of all backhaul links, $P_{\text{F}_{n,m}}$, is set to 0.

Figure 11, The probability of a certain TN n staying silent, P^{S}_{n}, vs. normalized distance, $\frac{d}{R}$, for *a)* JT scheme, *b)* CS scheme. **Cluster size** $=$ **2**, and the UEs advance towards the cluster center. The LFP of the backhaul links, P_{F}, is set to 0.1.

Figure 12, The probability of a certain TN n staying silent, P^{S}_{n}, vs. normalized distance, $\frac{d}{R}$, for *a)* JT scheme, *b)* CS scheme. **Cluster size** $=$ **3**, and the UEs advance towards the cluster center. The LFP of the backhaul links, P_{F}, is set to 0.1.

Figure 13, The average sum rate of the cluster, $\overline{C}$, vs. normalized distance, $\frac{d}{R}$, for , *a)* JT scheme, *b)* CS scheme. **Cluster size** $=$ **2**, and the UEs advance towards the cluster center. The LFP of the backhaul links, P_{F}, is set to 0.1.

Figure 14, The average sum rate of the cluster, $\overline{C}$, vs. normalized distance, $\frac{d}{R}$, for , *a)* JT scheme, *b)* CS scheme. **Cluster size** $=$ **3**, and the UEs advance towards the cluster center. The LFP of the backhaul links, P_{F}, is set to 0.1.

Figure 15, The average sum rate of the cluster, $\overline{C}$ vs. backhaul LFP, P_{F}, for *a)* JT scheme, *b)* CS scheme. **Cluster size** $=$ **2**, and the normalized distance, $\frac{d}{R}$, of the UEs from the cell centers is 0.4.

Figure 16, The average sum rate of the cluster, $\overline{C}$ vs. backhaul LFP, P_{F}, for *a)* JT scheme, *b)* CS scheme. **Cluster size** $=$ **3**, and the normalized distance, $\frac{d}{R}$, of the UEs from the cell centers is 0.4.

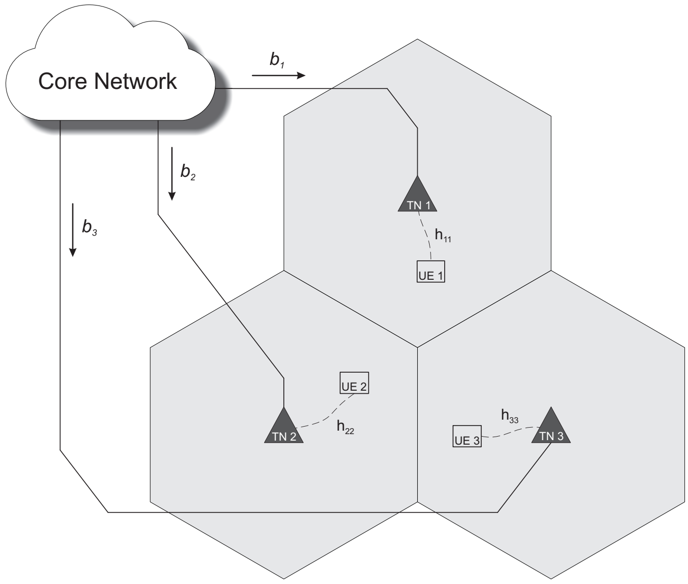

Figure 1. Single cell transmission. Traditional single cell transmission, with no cooperation between the TNs, is used as a baseline for performance evaluation.

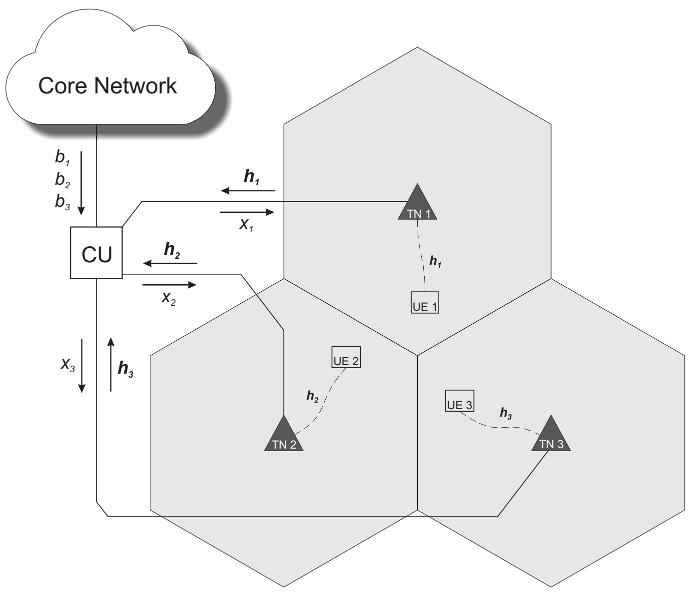

Figure 2. Centralized CoMP architecture. Under the centralized CoMP architecture the TNs forward CSI to a control unit, that applies precoding or makes scheduling decisions.

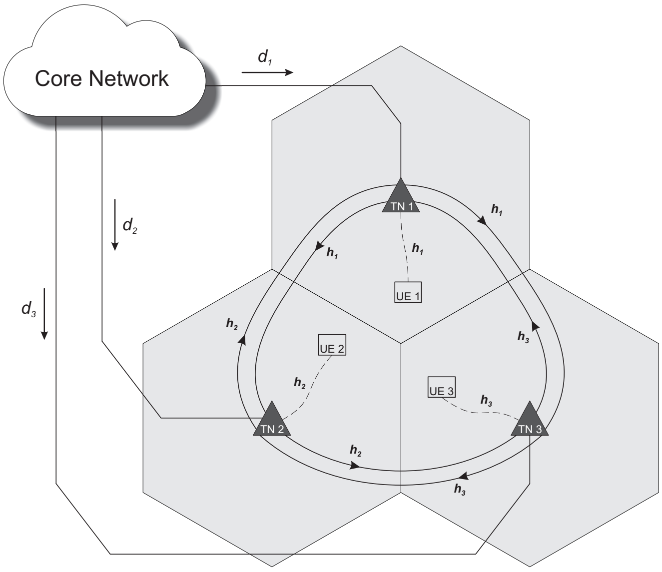

Figure 3. Semi-distributed CoMP architecture. Under the semi-distributed CoMP architecture each TNs acts as a control unit, local CSI is shared between the cooperating TNs.

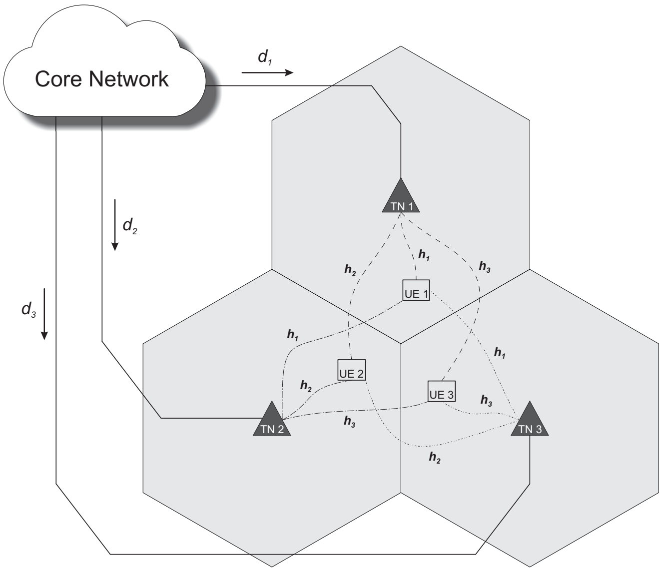

Figure 4. Fully distributed CoMP architecture. Under the fully distributed CoMP architecture each TNs acts as a control unit, all CSI is obtained directly from the UEs by broadcast.

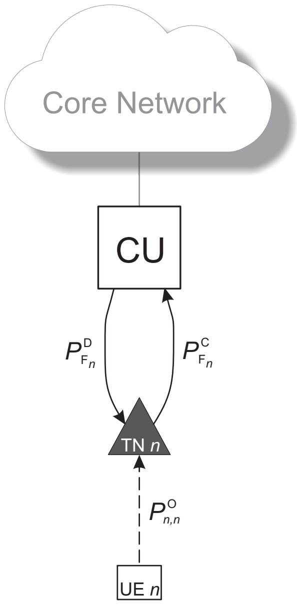

Figure 5. Relevant LFPs under centralized architecture. The individual LFPs of the backhaul network and control channels, that are taken into account during reliability analysis under centralized architecture.

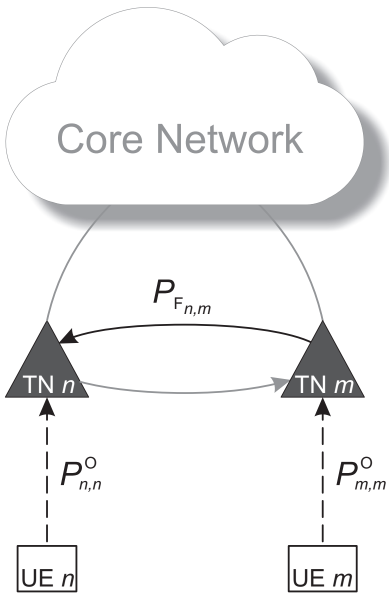

Figure 6. Relevant LFPs under semi-distributed architecture. The individual LFPs of the backhaul network and control channels, that are taken into account during reliability analysis under the semi-distributed architecture.

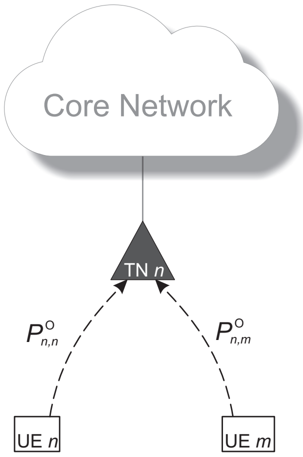

Figure 7. Relevant LFPs under fully distributed architecture. The individual LFPs of the backhaul network and control channels, that are taken into account during reliability analysis under the fully distributed architecture.

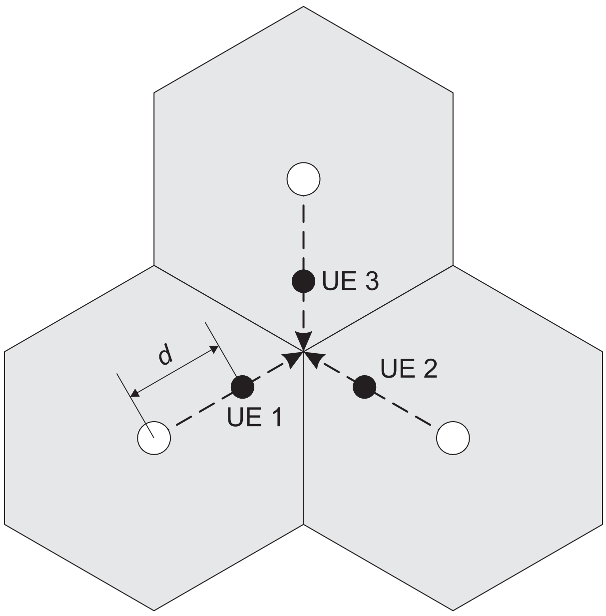

Figure 8. The simulated movement of the UEs, with cluster size $= 3$, considered in numerical performance evaluation. As the UEs approach the cluster center, the LFP between them and the TNs grows, impeding CSI feedback. Heightened interference also hampers data transmission.

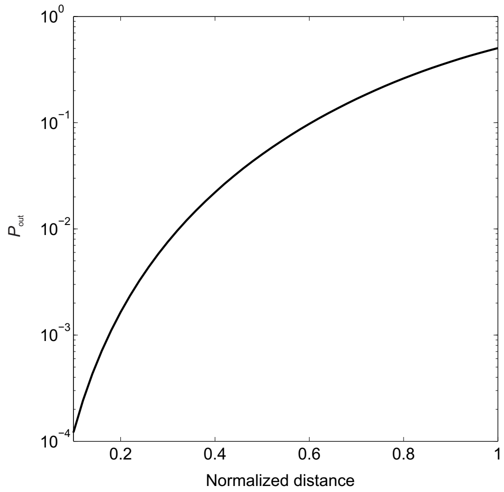

Figure 9. The LFP of the control channel over the access link used for CSI feedback, P_{out}, vs. normalized distance, $\frac{d}{R}$, between UE n and its serving TN n. It is assumed that the control channels are orthogonal for different users.

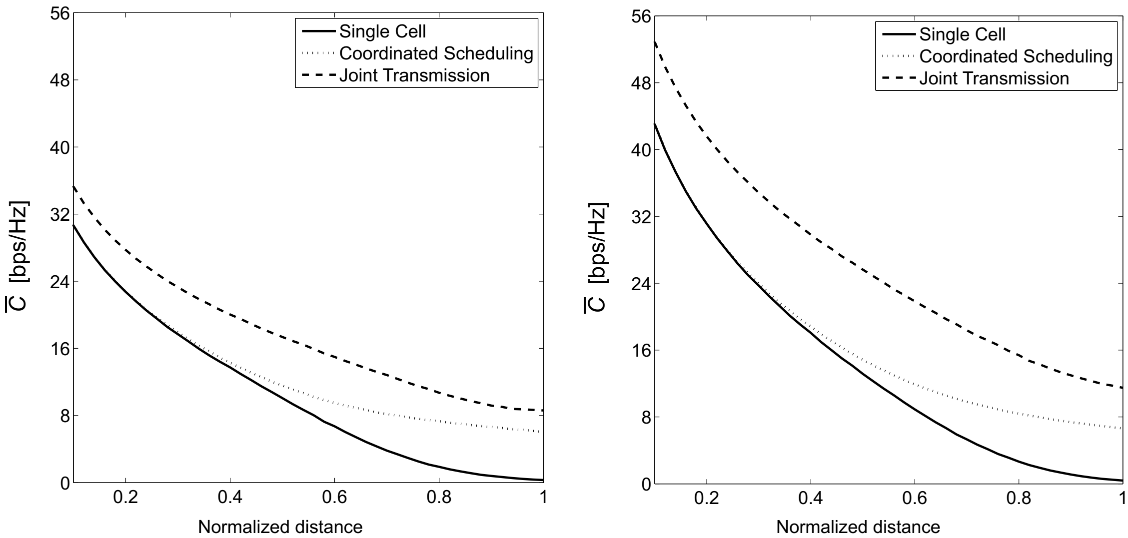

Figure 10. The average sum rate of the cluster, $\overline{C}$, vs. normalized distance, $\frac{d}{R}$, for *a)* Cluster size $=$ 2, *b)* Cluster size $=$ 3. It is assumed that the control channels are completely reliable, i.e., the LFP of all access links, $P^{\text{O}}_{n,m}$, and the LFP of all backhaul links, $P_{\text{F}_{n,m}}$, is set to 0.

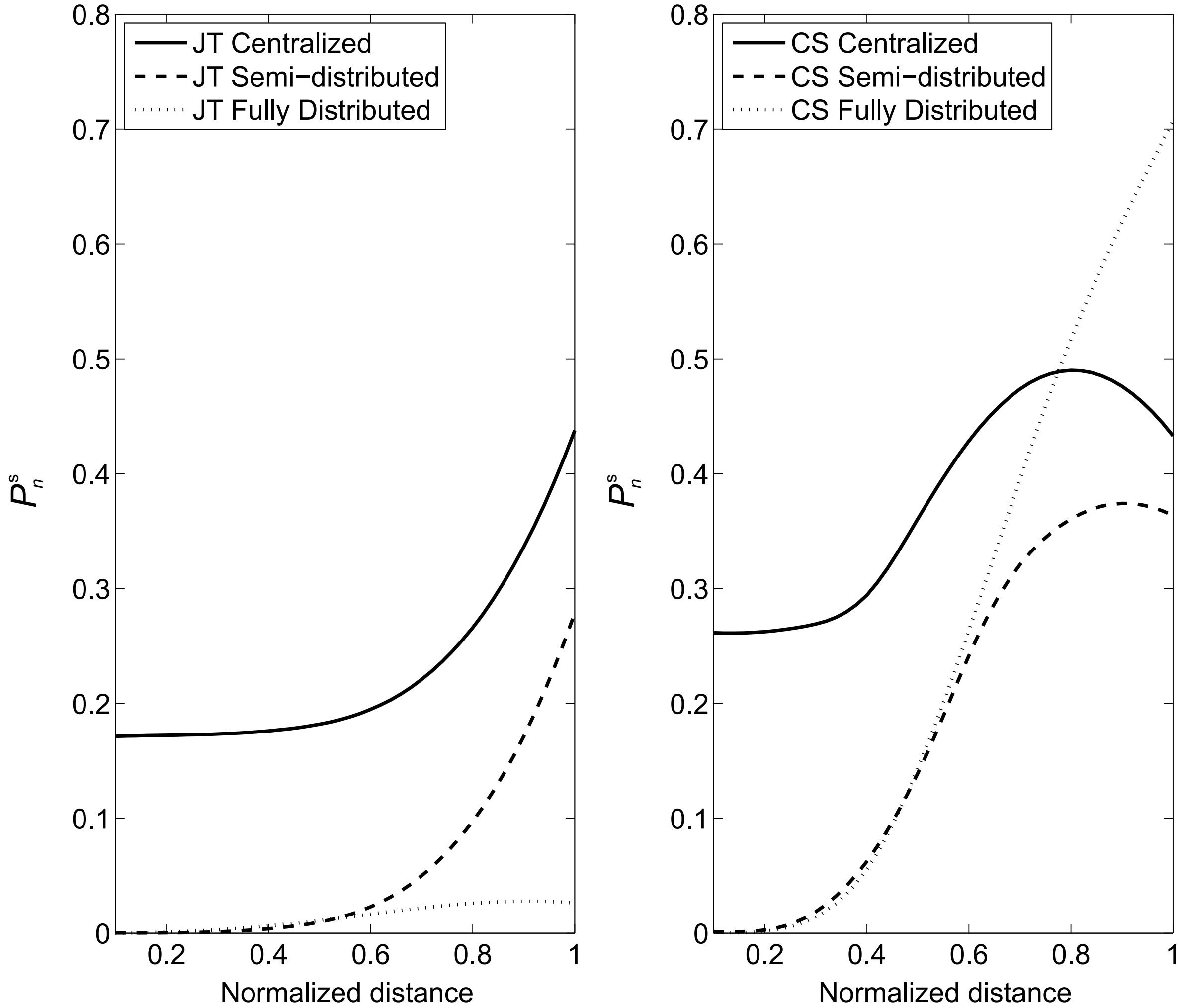

Figure 11. The probability of a certain TN n staying silent, P_n^{S}, vs. normalized distance, $\frac{d}{R}$, for *a)* JT scheme, *b)* CS scheme. **Cluster size** $= \mathbf{2}$, and the UEs advance towards the cluster center. The LFP of the backhaul links, P_{F}, is set to 0.1.

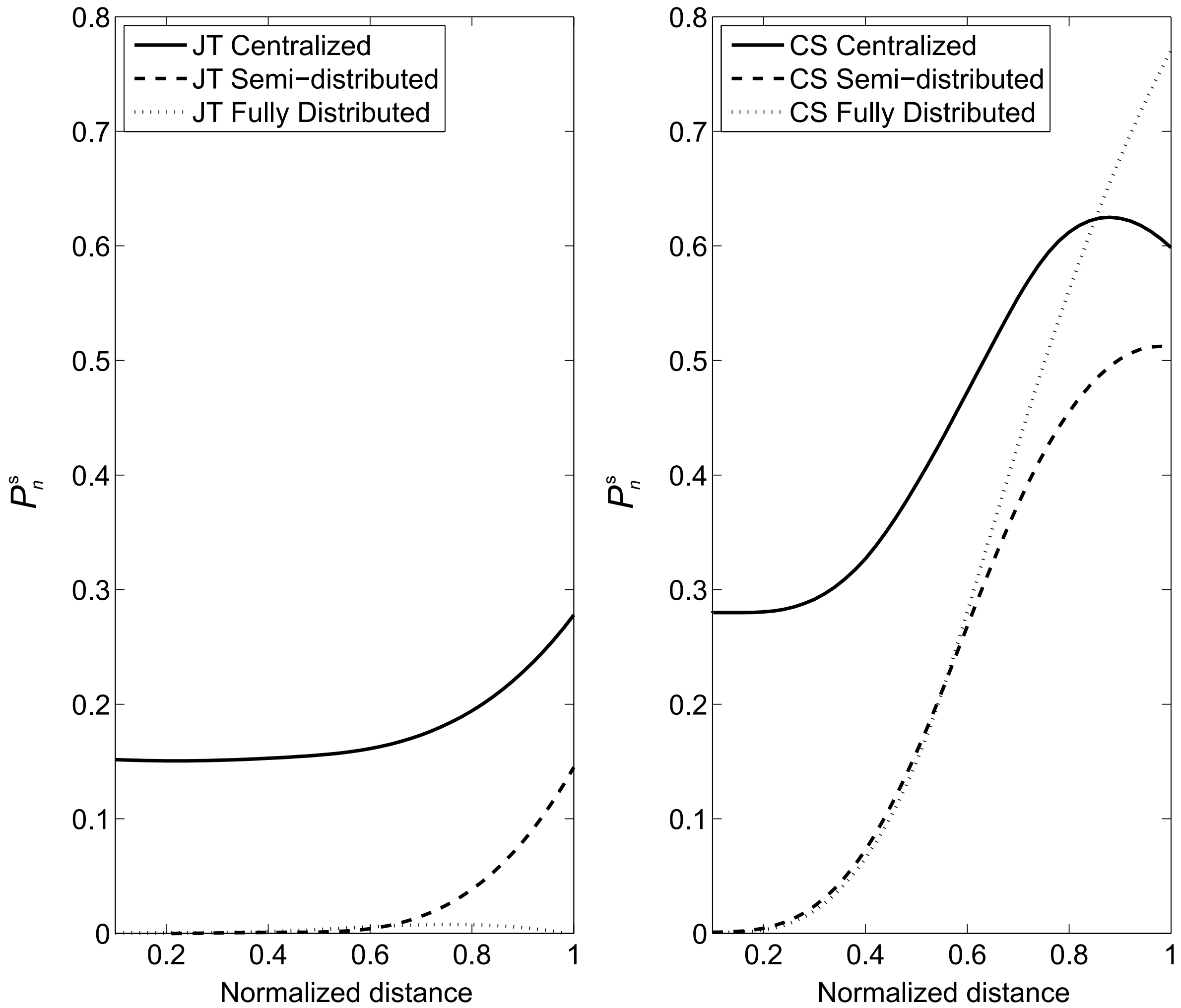

Figure 12. The probability of a certain TN n staying silent, P_n^{S}, vs. normalized distance, $\frac{d}{R}$, for *a)* JT scheme, *b)* CS scheme. **Cluster size** $= \mathbf{3}$, and the UEs advance towards the cluster center. The LFP of the backhaul links, P_{F}, is set to 0.1.

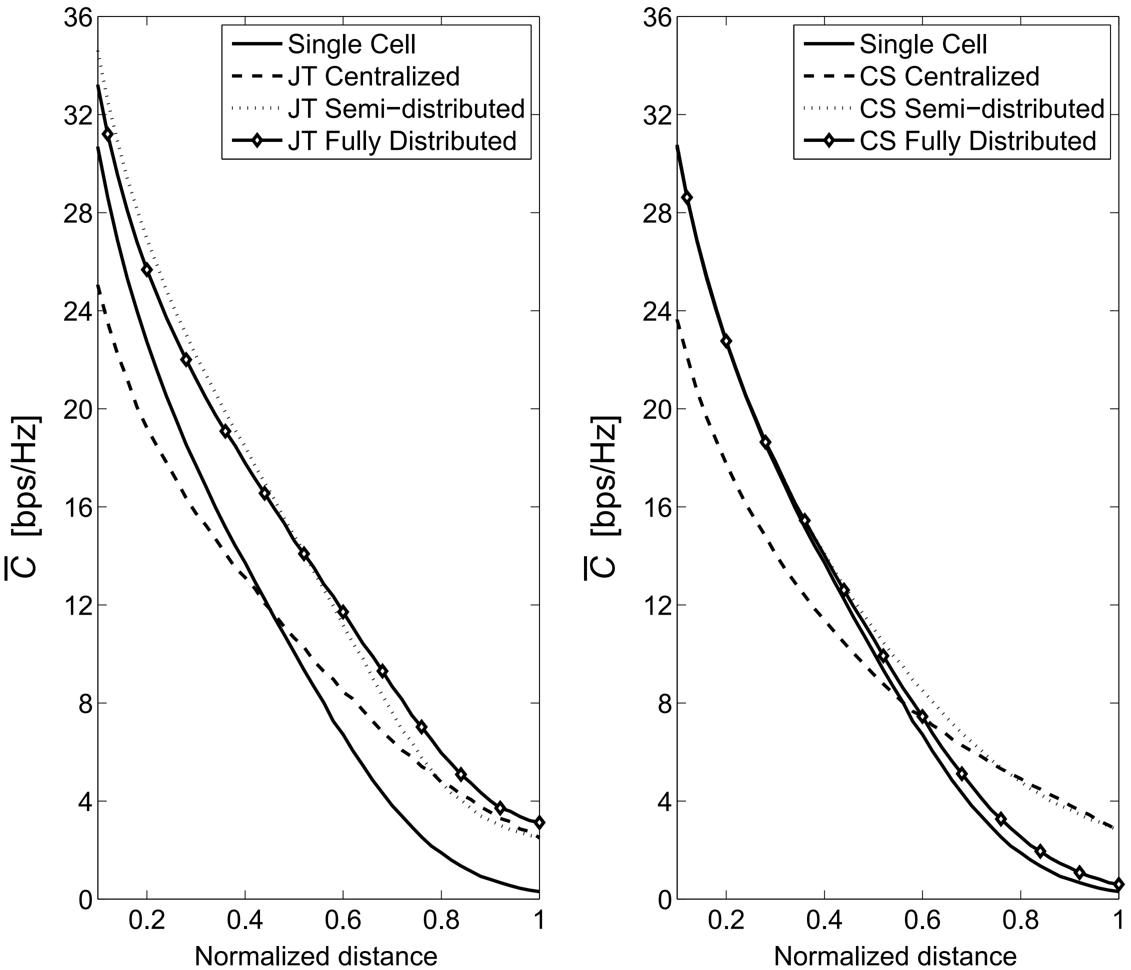

Figure 13. The average sum rate of the cluster, $\overline{C}$, vs. normalized distance, $\frac{d}{R}$, for , *a)* JT scheme, *b)* CS scheme. **Cluster size** $= \mathbf{2}$, and the UEs advance towards the cluster center. The LFP of the backhaul links, P_{F}, is set to 0.1.

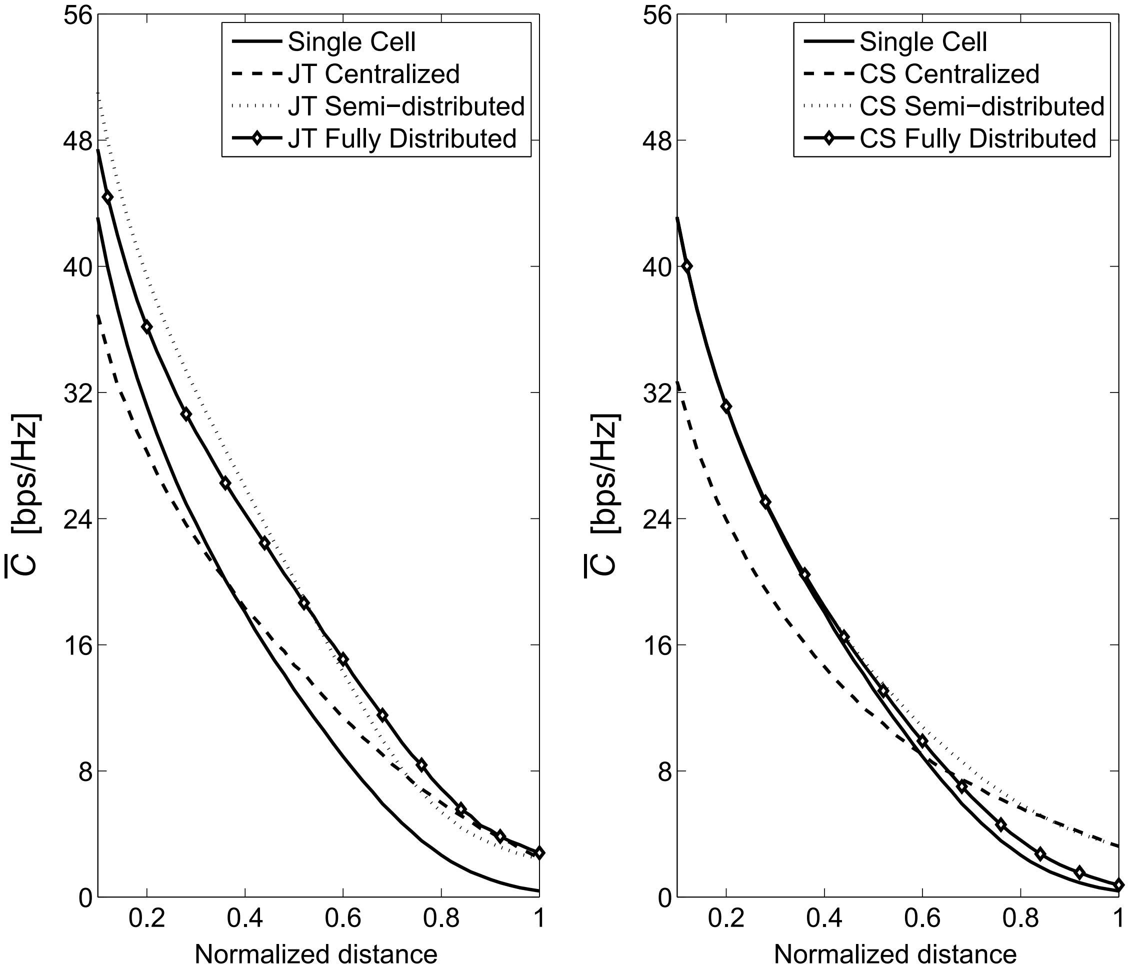

Figure 14. The average sum rate of the cluster, $\overline{C}$, vs. normalized distance, $\frac{d}{R}$, for , *a)* JT scheme, *b)* CS scheme. **Cluster size** $= \mathbf{3}$, and the UEs advance towards the cluster center. The LFP of the backhaul links, P_{F}, is set to 0.1.

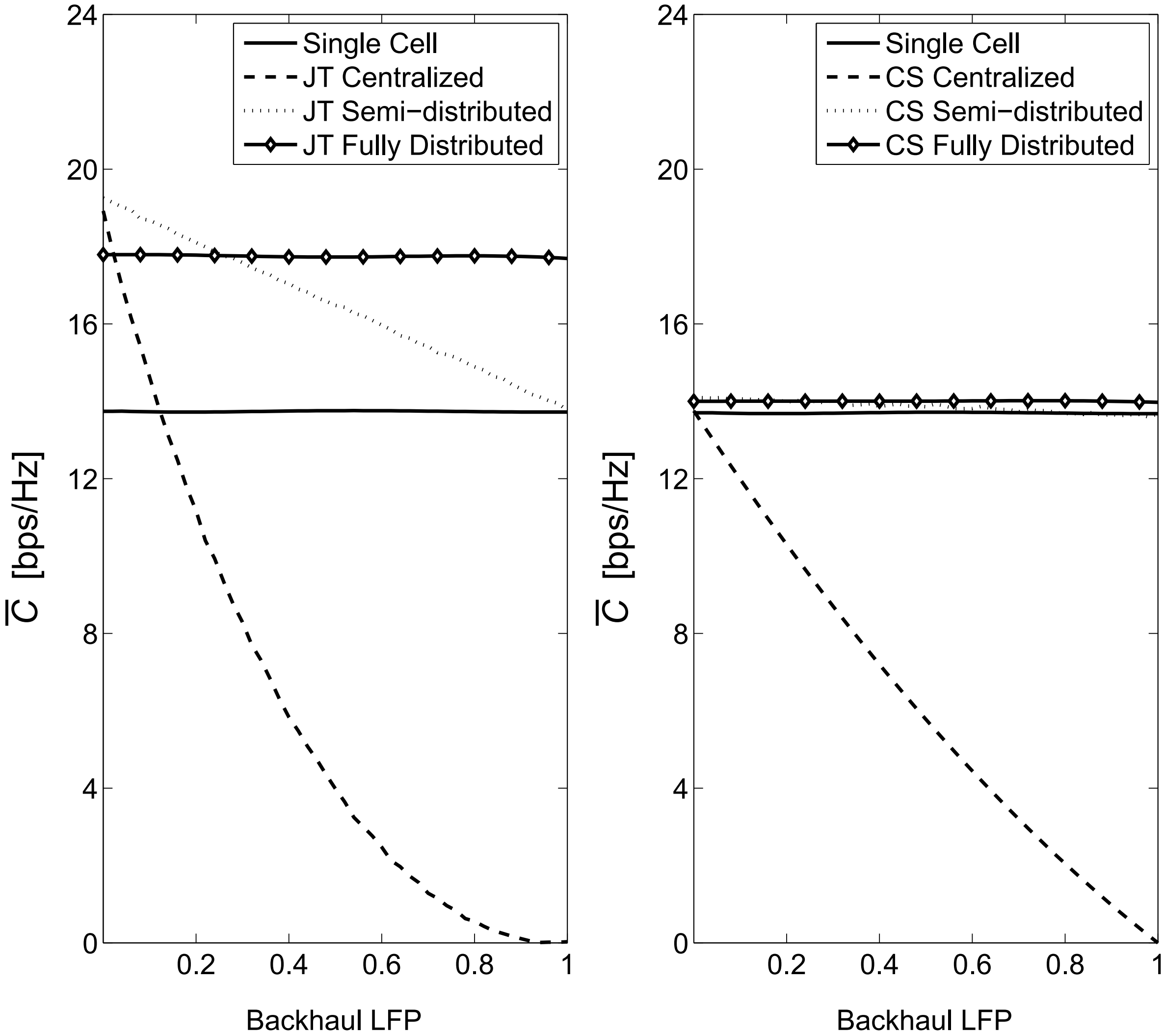

Figure 15. The average sum rate of the cluster, $\overline{C}$ vs. backhaul LFP, P_{F}, for *a)* JT scheme, *b)* CS scheme. **Cluster size** $= \mathbf{2}$, and the normalized distance, $\frac{d}{R}$, of the UEs from the cell centers is 0.4.

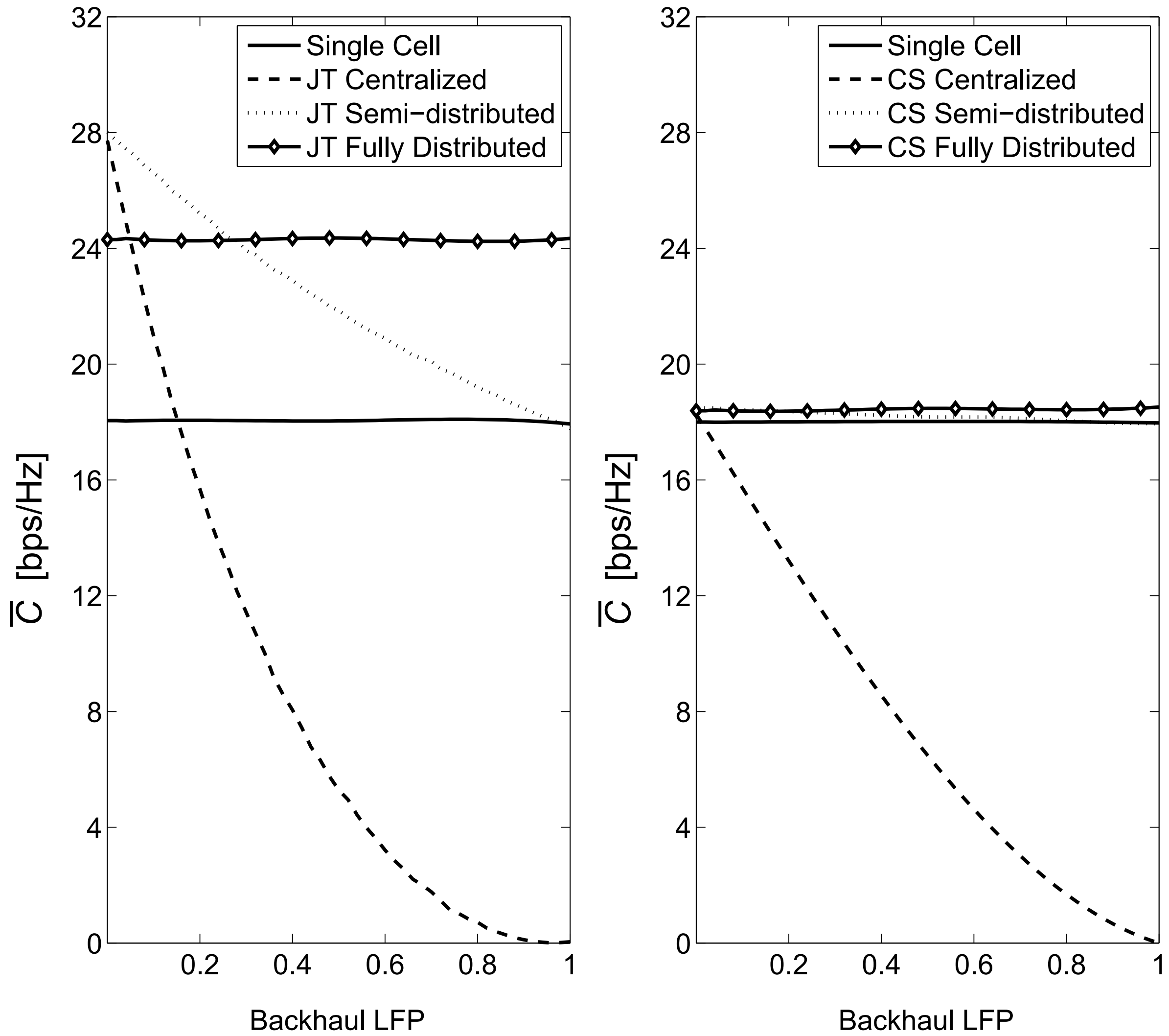

Figure 16. The average sum rate of the cluster, $\overline{C}$ vs. backhaul LFP, P_{F}, for *a)* JT scheme, *b)* CS scheme. **Cluster size** $= \mathbf{3}$, and the normalized distance, $\frac{d}{R}$, of the UEs from the cell centers is 0.4.